

# Zeroth-Order Regularized Optimization (ZORO): Approximately Sparse Gradients and Adaptive Sampling

HanQin Cai<sup>1</sup>, Daniel McKenzie<sup>1</sup>, Wotao Yin<sup>2,1</sup>, and Zhenliang Zhang<sup>2</sup>

<sup>1</sup>Department of Mathematics,  
University of California, Los Angeles, CA, USA.

<sup>2</sup>Damo Academy, Alibaba US,  
Seattle, WA, USA.

May 28, 2022

## Abstract

We consider the problem of minimizing a high-dimensional objective function, which may include a regularization term, using (possibly noisy) evaluations of the function. Such optimization is also called derivative-free, zeroth-order, or black-box optimization. We propose a new **Zeroth-Order Regularized Optimization** method, dubbed ZORO. When the underlying gradient is approximately sparse at an iterate, ZORO needs very few objective function evaluations to obtain a new iterate that decreases the objective function. We achieve this with an adaptive, randomized gradient estimator, followed by an inexact proximal-gradient scheme. Under a novel approximately sparse gradient assumption and various different convex settings, we show the (theoretical and empirical) convergence rate of ZORO is only logarithmically dependent on the problem dimension. Numerical experiments show that ZORO outperforms the existing methods with similar assumptions, on both synthetic and real datasets.

## 1 Introduction

Zeroth-order optimization, also known as derivative-free or black-box optimization, appears in a wide range of applications where either the objective function is implicit or the objective gradient is impossible or too expensive to compute. These applications include structured prediction (Taskar et al., 2005), reinforcement learning (Choromanski et al., 2018), bandit optimization (Flaxman et al., 2004; Shamir, 2013) optimal setting search in material science experiments (Nakamura et al., 2017), adversarial attacks on neural networks (Kurakin et al., 2016; Papernot et al., 2017), and hyper-parameter tuning (Snoek et al., 2012).

Formally, the goal of zeroth-order optimization is to solve the minimization problem:

$$\underset{x \in \mathcal{X} \subseteq \mathbb{R}^d}{\text{minimize}} f(x) \quad (1)$$

---

Email addresses: hqcai@math.ucla.edu (H.Q. Cai), mckenzie@math.ucla.edu (D. McKenzie), wotao.yin@alibaba-inc.com (W. Yin), and zhenliang.zhang@alibaba-inc.com (Z. Zhang).

with access to (potentially noisy) function evaluations only. These function evaluations are acquired through an *oracle*:

$$E_f(x) = f(x) + \xi, \quad (2)$$

where  $\xi$  is the unknown oracle noise. When we call the oracle with an input  $x$ , it returns  $E_f(x)$  in which  $\xi$  may or may not change every time. Zeroth-order methods are typically evaluated in terms of the number of required oracle queries.

One popular approach to zeroth-order optimization is to use oracle queries to estimate the gradient and then apply a first-order optimization method (Kiefer et al., 1952; Spall, 1998; Nesterov & Spokoiny, 2011). Generally speaking, gradient estimation based methods are favorable with convex objective models (Agarwal et al., 2010; Duchi et al., 2015; Wang et al., 2018), and also suitable with some non-convex models (Nesterov & Spokoiny, 2011; Ghadimi & Lan, 2013) and parallel optimization (Lian et al., 2016; Gu et al., 2018).

Nevertheless, these methods suffer from a mild curse of dimensionality. Compared with the analogous first-order methods, zeroth-order methods employing gradient estimators typically have a linear factor of the problem dimension,  $d$ , in their oracle complexity (Jamieson et al., 2012; Duchi et al., 2015). This is problematic when  $d$  is very large.

To reduce query complexity in the high dimensional case, (Wang et al., 2018) and (Balasubramanian & Ghadimi, 2018) introduced methods that exploit *exact sparsity* in the gradients. That is,  $\nabla f(x)$  has only a few non-zero entries at any point  $x$ . Their methods enjoy a query complexity that is polynomially dependent on  $\log(d)$ —a significant saving in the high dimensional case. However, their exact sparsity assumption often fails to hold in practice. In fact, (Balasubramanian & Ghadimi, 2018) has no empirical results, and (Wang et al., 2018) provides only experiments on synthetic datasets.

*Approximate sparsity* is a more practical assumption. For example, in hyper-parameter tuning, the performance is often sensitive to only a few hyper-parameters, so they tend to carry more significant weights in gradients. But, less-sensitive ones also have non-zero weights and need to be tuned. Furthermore, gradient sparsity varies during optimization, so methods assuming a fixed level of sparsity have limited practical use. Good methods need to explore the opportunity offered by sparse gradients when they are present and still work even when gradients are not sparse.

In this work, we propose a new method, which we coin ZORO, for high dimensional *regularized* zeroth-order optimization problems:

$$\underset{x \in \mathbb{R}^d}{\text{minimize}} F(x) := f(x) + r(x), \quad (3)$$

where  $r(x)$  is an *explicit* proximal function that helps encode prior information about the solution. (We access  $f(x)$  only implicitly through an oracle.) ZORO exploits the exact sparse gradient assumption and a more flexible *approximately sparse* gradient assumption. Moreover, ZORO employs a novel *adaptive sampling* strategy for improved gradient estimation. Both noise-free oracles and *adversarially noisy* oracles are studied. Comprehensive analysis are provided for the proposed method under different settings.

## 1.1 Related work, contribution, and notation

Arguably, the first methods to employ zeroth order gradient estimators within a gradient-based optimization method are FDSA (Kiefer et al., 1952) and SPSA (Spall, 1998). SPSA was com-

prehensively analyzed in (Nesterov & Spokoiny, 2011)<sup>1</sup> where it was shown that after  $T$  oracle queries,  $f(x_T) - \min f \leq O(d/T)$  for noise-free oracles, and  $\mathbb{E}[f(x_T) - \min f] \leq O(d/\sqrt{T})$  for stochastic oracles with unspecified dependence on the stochasticity:  $E_f(x) = F(x, \xi)$ , but satisfying  $\mathbb{E}[F(x, \xi)] = f(x)$ . This convergence rate was improved to  $O(\sqrt{d/T})$  in (Ghadimi & Lan, 2013), and this rate is also achieved in (Lian et al., 2016). In (Jamieson et al., 2012), it is shown that for strongly convex  $f(x)$  and oracle of the form (2) with zero-mean noise, the zeroth order optimization problem is in  $\Omega(\sqrt{d/T})$ . Thus, the rate achieved in (Ghadimi & Lan, 2013; Lian et al., 2016) is essentially optimal without placing further assumptions on  $f(x)$ .

(Wang et al., 2018) first proposed the exact sparse gradient assumption, as well as a gradient estimator exploiting the assumption. Using this estimator in a mirror descent scheme and assuming zero-mean oracle noise, a convergence rate of  $O((s/T)^{1/3} \log(d))$  was shown, where  $\|\nabla f(x)\|_0 \leq s$  for all  $x$ . The sparse gradient assumption was also used in (Balasubramanian & Ghadimi, 2018), where a projected gradient descent scheme using carefully chosen step sizes was advertised as achieving a convergence rate of  $O((s/T)^{1/2} \log(d))$ . However, their analysis implicitly requires that the support of  $\nabla f(x)$  is *fixed*, which is a more stringent requirement than an uniform bound on the sparsity of gradients.

We also mention several recent papers (Liu et al., 2018, 2019; Chen et al., 2019), which propose zeroth-order versions of ADMM, signSGD and Adam, respectively. Finally, for a comprehensive overview of zeroth-order optimization methods, we refer the interested readers to the recent survey article (Larson et al., 2019).

**Contributions:** The main innovations of this paper are:

- (i) We extend the assumption of exact gradient sparsity to *approximate gradient sparsity*, and provide improved query complexity bounds for the noise-free oracle case (see Corollary 5.2). We do *not* assume the support of large nonzero entries remain the same across iterations.
- (ii) We introduce the notion of restricted strong convexity to zeroth-order optimization, and show that under this assumption, ZORO achieves *linear convergence* in the noise-free case with *adaptive query radius* (see Corollary 5.2).
- (iii) We study *regularized* zeroth-order optimization ((3)). To the best of our knowledge, the only other paper to consider this problem is (Liu et al., 2018), but here we combine this problem with sparse gradients.
- (iv) We consider *adversarial* (i.e., bounded but arbitrary) oracle noise. This is a different paradigm to the stochastic noise considered in (Wang et al., 2018; Balasubramanian & Ghadimi, 2018); hence our convergence results have a different flavor. Specifically, we show  $O(s \log(d)/T)$  convergence, in both the regularized and non-regularized case, to a certain error horizon, beyond which no further decrease in objective function value is possible (see Theorems 5.6 and 5.7). When  $f(x)$  is restricted strongly convex, we improve this to a *linear convergence* rate, again up until a certain error horizon (see Theorem 5.6).
- (v) To improve practicality, we develop a novel adaptive sampling strategy that exploits approximate gradient sparsity when it is present and still works if it is not. If all sampled gradients are approximately sparse, the above sample complexities remain valid; otherwise, the strategy

---

<sup>1</sup>Which later appeared as (Nesterov & Spokoiny, 2017).

takes around  $d$  samples in each step and has a complexity no worse than those of existing methods.

- (vi) Finally, we successfully applied ZORO to some real-world applications, *e.g.*, asset risk management (see Section 6.2) and sparse adversarial attacks on ImageNet (see Section 6.3). In contrast, the previous zeroth-order work with sparse gradient setting provides numerical results on synthetic datasets only.

**Notation:** For any vector or matrix,  $\|\cdot\|_0$  counts the non-zero entries;  $\|\cdot\|_1$  and  $\|\cdot\|_2$  denote the entrywise  $\ell_1$ -norm and  $\ell_2$ -norm, respectively. The gradient and Hessian of function  $f$  are denoted by  $\nabla f$  and  $\nabla^2 f$ , respectively. We shall frequently use  $\mathbf{g} := \nabla f(x)$  when the point,  $x$ , in question is clear. For ease of presentation, we also write  $\min f := \min\{f(x) : x \in \mathbb{R}^d\}$  and  $e_k := f(x_k) - \min f$ , where  $x_k$  is the  $k$ -th iteration point of ZORO. Moreover,  $[x]_{(s)}$  denotes the best  $s$ -sparse approximation to vector  $x$  while  $|x|_{(i)}$  denotes the  $i$ -th largest-in-magnitude component of  $x$ .

## 2 Problem setup

Firstly, we present the assumptions on the sparse gradients.

**Assumption 1** (Sparse gradients). We consider three types of sparsity for the gradients:

- 1.a (Exact sparsity). The gradients of  $f$  are *exactly  $s$ -sparse* if  $\|\nabla f(x)\|_0 \leq s_{\text{exact}}$  for all  $x \in \mathbb{R}^d$ .
- 1.b (Approximate sparsity). The gradients of  $f$  are *approximately  $s$ -sparse* if there exists a small numerical constant  $\psi$ , such that  $\|\nabla f(x) - [\nabla f(x)]_{(s)}\|_2 \leq \psi \|\nabla f(x)\|_2$  for all  $x \in \mathbb{R}^d$ .
- 1.c (Compressibility). The gradients of  $f$  are *compressible* if there exists a  $p \in (0, 1)$  such that  $|\nabla f(x)|_{(i)} \leq \|\nabla f(x)\|_2 i^{-1/p}$ .

Assumption 1.a is standard in the prior literature (Wang et al., 2018; Balasubramanian & Ghadimi, 2018). Essentially, Assumption 1.b states that there exist no more than  $s$  significant coordinates in  $\nabla f(x)$  for any  $x$ , and the tail of  $s$ -sparse approximation is relatively small in terms of  $\ell_2$ -norm. We can also view 1.a as a special case of 1.b by taking  $\psi = 0$ . Although the sparsity bound is uniform at all points, we emphasize that the support (or significant coordinates) of the gradients can be different among different points. The shift of gradient support indeed happens in applications; for instance, in hyper-parameter tuning, different subsets of hyper-parameters may be sensitive at each tuning stage.

Assumption 1.c does not specify support size  $s$ . But we can easily show that it implies

$$\|\nabla f(x) - [\nabla f(x)]_{(s)}\|_1 \leq \left(\frac{1}{p} - 1\right)^{-1} \|\nabla f(x)\|_2 s^{1-1/p} \quad (4)$$

$$\|\nabla f(x) - [\nabla f(x)]_{(s)}\|_2 \leq \left(\frac{2}{p} - 1\right)^{-1/2} \|\nabla f(x)\|_2 s^{1/2-1/p}; \quad (5)$$

see, for example, (Needell & Tropp, 2009, Section 2.5).

Furthermore, we also make the following assumption on the Hessian matrix of  $f$ , which is needed *only* when the oracle is noisy.

**Assumption 2** (Bounded Hessian). Let  $f$  be twice differentiable. Then there exists a constant  $H$  such that  $\|\nabla^2 f(x)\|_1 \leq H$  for all  $x \in \mathbb{R}^d$ .

This assumption is also common in the literature (Wang et al., 2018). Next, we present a standard assumption on the existence of minimizers and the smoothness of  $f$ .

**Assumption 3** (Non-empty solution set and Lipschitz continuous gradients). (i) The solution set of  $F$  is non-empty. (ii) For any  $x, y \in \mathbb{R}^d$ , we have that  $\|\nabla f(x) - \nabla f(y)\|_2 \leq L\|x - y\|_2$  for some constant  $L$ .

We emphasize that we are not assuming that we have access to  $\nabla f$ , only that the Lipschitz property holds for  $\nabla f$ . Next, we present the assumption on our noise model.

**Assumption 4** (Adversarially noisy oracle). The oracle noise  $\xi$  is bounded:  $\|\xi\|_2 \leq \sigma$ .

We do not assume the noise is zero-mean; nor do we assume its probability distribution is known.

Our analysis considers several different settings of regularized objective function  $F$ , involving convex and restricted strongly convex components. We provide the definitions of convexity and restricted strongly convexity, as well as the standard definition of coercivity.

**Definition 1** (Convexity). A function  $h$  is *convex* if

$$h(tx + (1 - t)y) \leq th(x) + (1 - t)h(y) \quad (6)$$

for all  $x, y \in \mathbb{R}^d$  and  $t \in [0, 1]$ . Additionally, if  $h$  is differentiable, then (6) is equivalent to

$$h(y) \geq h(x) + \nabla h(x)^\top (y - x) \quad (7)$$

for all  $x, y \in \mathbb{R}^d$ .

Although the underlying  $f$  is differentiable in our setting, we still provide the definition of convexity here, since the regularizer  $r$  can be convex but non-differentiable.

**Definition 2** (Restricted strong convexity). A function  $h$  is *restricted  $\nu$ -strongly convex* if

$$h(x) - \min h \geq \nu \|x - P_*(x)\|_2^2 \quad (8)$$

for all  $x \in \mathbb{R}^d$ , where  $P_*(\cdot)$  is a projection operator onto the solution set defined by  $P_*(x) := \operatorname{argmin}_{y \in \text{solution set of } h} \|y - x\|_2$ .

One can see Definition 2 is indeed weaker than the commonly used strong convexity. We refer the interested readers to (Schöpfer, 2016; Zhang, 2017) for more results.

**Definition 3** (Coercivity). 1. A function  $h : \mathbb{R}^d \rightarrow \mathbb{R}$  is *coercive* if  $\lim_{\|x\|_2 \rightarrow \infty} h(x) = +\infty$ .

2. More generally, a function  $h : \mathbb{R}^d \rightarrow \mathbb{R}$  is *coercive with respect to  $g : \mathbb{R}^d \rightarrow \mathbb{R}$*  if, for any  $\{x\}_{k=1}^\infty$  satisfying  $\lim_{k \rightarrow \infty} g(x_k) = +\infty$ , we also have  $\lim_{k \rightarrow \infty} h(x_k) = +\infty$ .

---

**Algorithm 1** Zeroth Order Regularized Optimization Method (ZORO)

---

1: **Input:**  $x_0$ : initial point;  $s$ : gradient sparsity level as in Assumption 1.b;  $\alpha$ : step size;  $\beta$ : query radius parameter;  $\delta_0$ : initial query radius,  $\phi$ : error tolerance for OppGradEst (*optional*).  
2:  $m \leftarrow c_2 s \log(d/s)$   
3: **for**  $i = 1$  **to**  $m$  **do**  
4:   Generate Rademacher random vector  $z_i$ .  
5: **end for**  
6: **for**  $k = 0$  **to**  $K$  **do**  
7:    $\begin{cases} \hat{\mathbf{g}}_k \leftarrow \text{GradientEstimation}(x_k, s, \delta_k, \{z_i\}_{i=1}^m) & \text{or,} \\ (\hat{\mathbf{g}}_k, \{z_i\}_{i=1}^m) \leftarrow \text{OppGradEst}(x_k, \hat{S}_{k-1}, \delta_k, \{z_i\}_{i=1}^m, \phi) \end{cases}$   
8:    $x_{k+1} \leftarrow \text{prox}_{\alpha r}(x_k - \alpha \hat{\mathbf{g}}_k)$   
9:    $\delta_{k+1} \leftarrow \begin{cases} \beta \|\hat{\mathbf{g}}_k\|_2 & \text{Noise-free oracle case and } r(x) = 0 \\ C/k^{1.1} & \text{Noise-free oracle and } r(x) \neq 0 \\ \sqrt{2\sigma/H} & \text{Noisy oracle case} \end{cases}$   
10:    $\hat{S}_k \leftarrow \text{supp}(\hat{\mathbf{g}}_k)$   
11: **end for**  
12: **Output:**  $x_K$ : minimizer of (3).

---

### 3 Proposed method

In this section, we present the proposed novel method for solving regularized minimization problem (3), coined Zeroth-Order Regularized Optimization (ZORO).

Proximal-gradient methods are popular and well studied for first-order regularized optimization problems. For handling the regularized zeroth-order problem, we apply gradient descent with the estimated gradient, and then employ the proximal operator, which is defined as

$$\text{prox}_{\alpha r}(y) := \underset{x \in \mathbb{R}^d}{\text{argmin}} r(x) + \frac{1}{2\alpha} \|x - y\|_2^2. \quad (9)$$

Furthermore, when estimating the gradient, we provide different versions of query radius for noise-free and noisy oracle cases. In either case, our query radius strategy ensures overall good sampling quality by tuning only one parameter. In summary, ZORO is proximal-gradient descent with an exact proximal operator but inexact gradients. We formalize ZORO as Method 1, and its convergence will be analyzed in Section 5 under different settings.

#### 3.1 Gradient estimation

Following (Wang et al., 2018), in this section we show how the sparse gradient estimation problem can be posed as a sparse recovery problem. Specifically, choose a query number  $m$  and a sampling radius  $\delta$ , and let  $\{z_i\}_{i=1}^m \in \mathbb{R}^d$  be Rademacher random vectors. That is:

$$(z_i)_j = \begin{cases} +1 & \text{with probability } 1/2, \\ -1 & \text{with probability } 1/2. \end{cases} \quad (10)$$

for all  $i = 1, \dots, m$  and  $j = 1, \dots, d$ . To construct each measurement (in the compressed sensing sense) we make two oracle queries, at  $x$  and at  $x + \delta z_i$ , to obtain  $E_f(x)$  and  $E_f(x + \delta z_i)$ . Then the

measurements can be defined as

$$y_i = \frac{1}{\sqrt{m}} \frac{E_f(x + \delta z_i) - E_f(x)}{\delta}. \quad (11)$$

which are (noisy) finite difference approximations to the directional derivative in the directions  $z_i$ . We present this sampling procedure as Algorithm 2.

**Lemma 3.1.** *If Assumptions 2 and 4 are satisfied, then*

$$y_i = \frac{1}{\sqrt{m}} z_i^\top \mathbf{g} + \frac{\mu_i}{\delta} + \delta \nu_i$$

with  $\mathbf{g} = \nabla f(x)$ ,  $|\mu_i| \leq 2\sigma/\sqrt{m}$ , and  $|\nu_i| \leq H/(2\sqrt{m})$ .

Thus, if  $f(x)$  also satisfies Assumption 1, one might hope to approximate  $\mathbf{g}$  via:

$$\hat{\mathbf{g}} = \underset{\mathbf{v} \in \mathbb{R}^d}{\operatorname{argmin}} \|Z\mathbf{v} - \mathbf{y}\|_2 \quad \text{such that } \|\mathbf{v}\|_0 \leq s, \quad (12)$$

where  $\mathbf{y} = [y_1, \dots, y_m]^\top$  and  $Z \in \mathbb{R}^{m \times d}$  is the *sensing matrix* whose  $i$ -th row is  $\frac{1}{\sqrt{m}} z_i^\top$ . We propose to solve Problem (12) approximately using CoSaMP (Needell & Tropp, 2009), and present the resulting gradient estimation procedure as Algorithm 3. In Theorem 3.2, we shall analyze the accuracy of this approach. Before proceeding, let us mention that an alternate approach to (12) could be to use LASSO:

$$\hat{\mathbf{g}} = \underset{\mathbf{v} \in \mathbb{R}^d}{\operatorname{argmin}} \frac{1}{2} \|Z\mathbf{v} - \mathbf{y}\|_2^2 + \lambda \|\mathbf{v}\|_1, \quad (13)$$

which is similar to the approach taken in (Wang et al., 2018). However, there are at least three reasons why a greedy approach such as CoSaMP could be preferable:

- (i) The LASSO estimator is typically biased (Fan & Li, 2001), while the CoSaMP estimator does not have this problem. This allows one to take (a constant factor) fewer oracle queries. Moreover, our analysis using CoSaMP allows for *adversarial noise*.
- (ii) CoSaMP is typically faster for small sparsity levels,  $s$ .
- (iii) Empirically, we have found that hand tuning the parameter  $\lambda$  is inefficient and it needs to be done dynamically to ensure convergence of main method (See Section 6).

**Theorem 3.2.** *Suppose that  $\{z_i\}_{i=1}^m$  are generated as described in Algorithm 1. Suppose further that Assumptions 1, 2 and 4 are satisfied. Then with probability at least  $1 - (s/d)^{O(s)}$ :*

$$\|\hat{\mathbf{g}} - \mathbf{g}\|_2 \leq (\psi + \rho^n) \|\mathbf{g}\|_2 + \frac{2\tau\sigma}{\delta} + \frac{\tau\delta H}{2},$$

for all  $x \in \mathbb{R}^d$ , where  $\hat{\mathbf{g}}$  denotes the output after  $n$  iterations of CoSaMP applied to problem (12). Here  $\rho < 1$  and  $\tau \approx 15$  are fixed numerical constants, and:

$$\psi = \begin{cases} 0 & \text{if } f(x) \text{ satisfies Assumption 1.a} \\ Cs^{1/2-1/p} & \text{if } f(x) \text{ satisfies Assumption 1.c.} \end{cases}$$

Note that  $C$  depends on  $p$  and  $\{z_i\}_{i=1}^m$ , but not on  $s$ .

---

**Algorithm 2** Sample

---

- 1: **Input:**  $x$ : current point;  $\delta$ : query radius;  $r$ ,  $\{z_i\}_{i=1}^r$ : sample number and directions.
  - 2: Sample at point  $x$ , obtain  $E_f(x)$ .
  - 3: **for**  $i = 1$  **to**  $r$  **do**
  - 4:   Sample at point  $x + \delta z_i$  to obtain  $E_f(x + \delta z_i)$ .
  - 5:    $y_i \leftarrow \frac{E_f(x + \delta z_i) - E_f(x)}{\delta}$
  - 6: **end for**
  - 7:  $\mathbf{y} \leftarrow [y_1, \dots, y_r]^\top$
  - 8: **Output:**  $\mathbf{y}$
- 

---

**Algorithm 3** Gradient Estimation

---

- 1: **Input:**  $x$ : current point;  $s$ : gradient sparsity level as in Assumption 1.b;  $\delta$ : query radius;  $\{z_i\}_{i=1}^m$ : sample directions.
  - 2:  $\mathbf{y} \leftarrow \frac{1}{\sqrt{m}} \text{Sample}(x, \delta, \{z_i\}_{i=1}^m)$
  - 3:  $\mathbf{Z} \leftarrow \frac{1}{\sqrt{m}} [z_1, \dots, z_m]^\top$
  - 4:  $\hat{\mathbf{g}} \approx \text{argmin}_{\|\mathbf{g}\|_0 \leq s} \|\mathbf{Z}\mathbf{g} - \mathbf{y}\|_2$    by CoSaMP
  - 5: **Output:**  $\hat{\mathbf{g}}$
- 

The proofs of Lemma 3.1 and Theorem 3.2 can be found in Appendix A. The exact values of  $\rho$  and  $\tau$  are given in (Foucart, 2012), while the exact form of  $C$  is given in Lemma A.5. Note that as  $p \in (0, 1)$  we can make  $\psi$  (almost) arbitrarily small by taking  $s$  to be larger. We point out that the error bound in Theorem 3.2 is universal, *i.e.* it holds *for all*  $x$  with probability  $1 - (s/d)^{O(s)}$ , and this probability is over the random draw of the  $\{z_i\}_{i=1}^m$ .

### 3.2 Opportunistic Sampling

To establish the convergence analysis for ZORO, we assume an uniform  $s$  for all  $x \in \mathbb{R}^d$  in Assumption 1.b. Moreover, we assume no relationship between the support of the gradient at  $x_k$ , *i.e.*  $\text{supp}(\mathbf{g}_k)$ , and  $\text{supp}(\mathbf{g}_{k+1})$ . In practice, neither of these need to hold. The number of significant gradient coordinates can change—in particular as  $x_k \rightarrow x_*$ , and so  $g_k \rightarrow 0$ , it tends to increase. Moreover,  $\text{supp}(\mathbf{g}_k) \approx \text{supp}(\mathbf{g}_{k-1})$  holds at times, and they may even be equal. Hence, we can make two modifications to Algorithm 3 to take advantage of these phenomena, when they arise. We present this as Algorithm 4. Informally, Algorithm 4 proceeds as:

1. First, we test if  $\text{supp}(\mathbf{g}_k) \subseteq \text{supp}(\mathbf{g}_{k-1})$ . We do this by taking  $s$  samples and solving a least squares problem with support restricted to  $\text{supp}(\mathbf{g}_{k-1})$  (see lines 2–4 of Algorithm 4). If the relative error in this solution is small, we terminate the algorithm and return this solution as  $\hat{\mathbf{g}}_k$ .
2. If Algorithm 4 does not terminate after the above, we run a variation of Gradient Estimation (see lines 8–10 of Algorithm 4) while reusing the  $s$  samples we have already taken. We check whether the solution arising from this is sufficiently accurate (line 11 of Algorithm 4).
3. Until a sufficiently accurate solution is found, we generate additional  $z_i$  and oracle queries  $E_f(x + \delta z_i)$ , while retaining our earlier samples. We estimate the gradient from these samples,



---

**Algorithm 4** Opportunistic Gradient Estimation (OppGradEst)

---

```

1: Input:  $x$ : current point;  $\hat{S}_{k-1}$ : support of  $\hat{\mathbf{g}}_{k-1}$ ;  $\delta$ : query radius;  $\{z_i\}_{i=1}^m$ : sample directions;
    $\phi$ : error tolerance.
2:  $s \leftarrow |\hat{S}_{k-1}|$ 
3:  $\mathbf{y} \leftarrow \text{Sample}(x, \delta, \{z_i\}_{i=1}^s)$ 
4:  $Z \leftarrow [z_1, \dots, z_s]^\top$ 
5:  $\hat{\mathbf{g}} \leftarrow \text{argmin}_{\mathbf{g}} \|Z\mathbf{g} - \mathbf{y}\|_2 \quad \text{s.t. } \text{supp}(\mathbf{g}) = \hat{S}_{k-1}$ 
6: if  $\|Z\hat{\mathbf{g}} - \mathbf{y}\|_2 / \|\mathbf{y}\|_2 \leq \phi$  then
7:   Terminate algorithm and output
8: end if
9:  $\mathbf{y} \leftarrow \frac{1}{\sqrt{m}}[\mathbf{y}; \text{Sample}(x, \delta, \{z_i\}_{i=s+1}^m)]$ 
10:  $Z \leftarrow \frac{1}{\sqrt{m}}[z_1, \dots, z_m]^\top$ 
11:  $\hat{\mathbf{g}} \approx \text{argmin}_{\|\mathbf{g}\|_0 \leq s} \|Z\mathbf{g} - \mathbf{y}\|_2 \quad \text{by CoSaMP}$ 
12: while  $\|Z\hat{\mathbf{g}} - \mathbf{y}\|_2 / \|\mathbf{y}\|_2 > \phi$  do
13:    $m^{\text{new}} \leftarrow m + \log(d/s)$ 
14:   Generate Rademacher random vectors  $z_{m+1}, \dots, z_{m^{\text{new}}}$ 
15:    $\mathbf{y} \leftarrow \frac{1}{\sqrt{m^{\text{new}}}}[\sqrt{m}\mathbf{y}; \text{Sample}(x, \delta, \{z_i\}_{i=m+1}^{m^{\text{new}}})]$ 
16:    $Z \leftarrow \frac{1}{\sqrt{m^{\text{new}}}}[\sqrt{m}Z^\top, z_{m+1}, \dots, z_{m^{\text{new}}}]^\top$ 
17:    $m \leftarrow m^{\text{new}}$  and  $s \leftarrow s + 1$ 
18:    $\hat{\mathbf{g}} \approx \text{argmin}_{\|\mathbf{g}\|_0 \leq s} \|Z\mathbf{g} - \mathbf{y}\|_2 \quad \text{by CoSaMP}$ 
19: end while
20: Output:  $\hat{\mathbf{g}}, \{z_i\}_{i=1}^m$ 

```

---

old and new, (see lines 12–17 of Algorithm 4) and check whether it is sufficiently accurate.

At worst, we make around  $d$  queries, which is no worse than the dense gradient estimators. This strategy provides us a safeguard even if the gradients become dense.

## 4 Inexact gradient descent

Recall the sequence produced by ZORO can be written as:

$$x_{k+1} = \text{prox}_{\alpha r}(x_k - \alpha \hat{\mathbf{g}}_k). \quad (14)$$

Note that if  $r(x) = 0$  (i.e., there is no regularization), then (14) reduces to (inexact) gradient descent:  $x_{k+1} = x_k - \alpha \hat{\mathbf{g}}_k$ . We defer all proofs for this section to Appendix B.

### 4.1 Convex analysis

We shall need some tightened bounds on convergence for inexact gradient descent.

In this and next section, constant  $R$ , as in  $\|x_k - P_*(x_k)\|_2 \leq R$  for all  $k$ , denotes a number depending only on the coercivity of  $f(x)$  and a growth condition described in Appendix B. See Theorem B.6 for more details.

**Theorem 4.1** (Sublinear convergence). *Suppose that  $f(x)$  is convex and satisfies Assumption 3.*

1. **Absolute bound<sup>2</sup>:** If  $\|\mathbf{g}_k - \hat{\mathbf{g}}_k\|_2 \leq \varepsilon_{\text{abs}}$ ,  $\alpha < 2/L$  and  $\|x_k - P_*(x_k)\|_2 \leq R$  for  $k = 1, \dots, K$ , then:

$$e_K \leq \max \left\{ \frac{e_0}{Ke_0/(c_3 R^2) + 2}, R\sqrt{c_4 \varepsilon_{\text{abs}}} \right\} \\ \sim \max \left\{ c_3 R^2 \cdot \frac{1}{K}, R\sqrt{\varepsilon_{\text{abs}}} \right\}.$$

2. **Relative bound:** If  $\|\mathbf{g}_k - \hat{\mathbf{g}}_k\|_2 \leq \varepsilon_{\text{rel}} \|\mathbf{g}_k\|_2$ ,  $\alpha < 2/L$  and  $\|x_k - P_*(x_k)\|_2 \leq R$  for all  $k$ , then:

$$e_k \leq \frac{e_0}{ke_0/(c_5 R^2) + 1} \sim c_5 R^2 \cdot \frac{1}{k}.$$

The constants  $c_3$ ,  $c_4$  and  $c_5$  are defined as in Lemma B.5.

We remark that the assumption  $\|x_k - P_*(x_k)\|_2 \leq R$  is rather strong. In Theorem B.6 we provided weaker sufficient conditions under which this holds.

## 4.2 Restricted strongly convex analysis

Finally, we present some useful results on inexact gradient descent when  $f(x)$  is restricted strongly convex. Note that part 1 of 4.2 is essentially Corollary 1 of (Zhang & Cheng, 2015). We include a proof in Appendix B for completeness.

**Theorem 4.2** (Linear convergence). *Suppose that  $f(x)$  is convex, restricted  $\nu$ -strongly convex and satisfies Assumption 3. Then:*

1. **Absolute bound:** If  $\|\mathbf{g}_k - \hat{\mathbf{g}}_k\|_2^2 \leq \varepsilon_{\text{abs}} \forall k$ , then

$$e_k \leq c_6^k e_0 + (1 - c_6)^{-1} c_7 \varepsilon_{\text{abs}}$$

$$\text{where } c_6 = \frac{4\alpha - 2\nu + \nu\alpha L}{4\alpha} \text{ and } c_7 = \frac{\alpha^2(2 + \alpha L)}{4\alpha}.$$

2. **Relative bound:** If  $\|\mathbf{g}_k - \hat{\mathbf{g}}_k\|_2 \leq \varepsilon_{\text{rel}} \|\mathbf{g}_k\|_2 \forall k$ , then

$$e_k \leq (1 - c_8)^k e_0$$

$$\text{where } c_8 = \frac{2\nu - \nu\alpha L - \nu\alpha^2 \varepsilon_{\text{rel}}^2 (2 + \alpha L)}{4\alpha}.$$

## 5 Convergence analysis for ZORO

In this section we present a variety of convergence results for ZORO, under different assumptions on  $f(x)$ ,  $r(x)$  and  $E_f(x)$ . For simplicity, in Sections 5.1 and 5.2 we shall assume ZORO is implemented using the simpler GradientEstimation Algorithm (Algorithm 3). We discuss how one might adapt these results to ZORO using OppGradEst (Algorithm 4) in Section 5.3.

---

<sup>2</sup>We use the symbol “ $\sim$ ” to keep only the leading term in the polynomial.

## 5.1 Noise-free oracle case

Here, we assume that the oracle is noise-free, *i.e.*  $\sigma = 0$  in Assumption 4. The main result of this section is that by choosing  $\delta_k$  adaptively, one can guarantee that  $\|\mathbf{g}_k - \hat{\mathbf{g}}_k\|_2 \leq \varepsilon_{\text{rel}} \|\mathbf{g}_k\|_2$  for all  $k$ , with high probability.

**Theorem 5.1.** *Suppose that  $f(x)$  satisfies Assumption 1 with  $\psi < \min \left\{ \frac{1-\alpha L}{2-\alpha L}, \frac{2-\alpha L}{4-\alpha L} \right\}$  and Assumption 3, and suppose further that  $\alpha < 1/L$ . Choose  $\varepsilon_{\text{rel}}$  and  $n$  such that:*

$$\psi + \rho^n < \varepsilon_{\text{rel}} < \min \left\{ \frac{1-\alpha L}{2-\alpha L}, \frac{2-\alpha L}{4-\alpha L} \right\},$$

and define:

$$\beta = \frac{2(\varepsilon_{\text{rel}} - \psi - \rho^n)(1 - L\alpha - \varepsilon_{\text{rel}}(2 - \alpha L))}{\tau H(1 - \varepsilon_{\text{rel}})}.$$

If  $\|\mathbf{g}_0 - \hat{\mathbf{g}}_0\|_2 \leq \varepsilon_{\text{rel}} \|\mathbf{g}_0\|_2$  and  $\delta_k < \beta \|\hat{\mathbf{g}}_{k-1}\|_2$ , then:

$$\|\mathbf{g}_k - \hat{\mathbf{g}}_k\|_2 \leq \varepsilon_{\text{rel}} \|\mathbf{g}_k\|_2$$

for all  $k$  with probability  $1 - (s/d)^{O(s)}$ .

We defer the proofs of this section to Appendix C, where we also discuss how to guarantee that  $\|\mathbf{g}_0 - \hat{\mathbf{g}}_0\|_2 \leq \varepsilon_{\text{rel}} \|\mathbf{g}_0\|_2$ . The constant  $\psi$  is discussed in Theorem 3.2 and defined in Lemma A.5. Note that this, combined with the results of Section 4 immediately yield the following:

**Corollary 5.2.** *Assume the hypotheses of Theorem 5.1. Let  $r(x) = 0$  and let  $x_K$  be the iterate returned by ZORO after making  $T$  oracle queries, where  $K = T/m$ .*

1. *If  $f(x)$  is convex and coercive then:*

$$e_K \leq \frac{c_5 e_0 R^2}{T e_0 / c_1 s \log(d/s) + c_5 R^2} = O\left(\frac{s \log(d/s)}{T}\right),$$

*with probability at least  $1 - (s/d)^{O(s)}$ .*

2. *If  $f(x)$  is convex and restricted  $\nu$ -strongly convex then:*

$$e_K \leq e_0 c_8^{T/c_1 s \log(d/s)}$$

*again with probability at least  $1 - (s/d)^{O(s)}$ .*

We now consider the case  $r(x) \neq 0$ .

**Theorem 5.3.** *Suppose that  $f(x)$  satisfies Assumptions 1.a and 3. If  $\delta_k < C/k^{1.1}$  and  $n$  is sufficiently large, then*

$$\|\mathbf{g}_k - \hat{\mathbf{g}}_k\|_2 \leq C\tau H/k^{1.1}$$

*for all  $k$ , with probability at least  $1 - (s/d)^{O(s)}$ .*

In Appendix C we discuss exactly how large  $n$  should be.

**Corollary 5.4.** Let  $F(x) := f(x) + r(x)$  with  $f(x)$  convex and satisfying Assumptions 1.a, 2 and 3 and  $r(x)$  a closed proper convex function. Choose  $\alpha = 1/L$  and let  $\{x_1, \dots, x_K\}$  be the iterates found by ZORO after making  $T$  total oracle queries, where  $K = T/m$ . Then:

$$\min_{k=1, \dots, K} F(x_k) - \min F \leq \frac{Ls \log(d/s)}{2T} \left( \|x_0 - P_*(x_0)\| + \frac{2E_\infty}{L} \right).$$

with probability at least  $1 - (s/d)^{O(s)}$ , where  $E_\infty = C\tau H \sum_{k=1}^{\infty} k^{-1.1}$ .

## 5.2 Noisy oracle case

Here we consider a noisy oracle, *i.e.*  $\sigma > 0$  in Assumption 4. For ease of comparison with (Wang et al., 2018) we consider the exact sparsity case (*i.e.*, Assumption 1.a).

**Theorem 5.5.** Suppose that  $f(x)$  satisfies Assumptions 1.a, 2 and 3,  $\delta_k = \delta = \sqrt{2\sigma/H}$  and  $n$  is sufficiently large. Then for all  $k$ :

$$\|\hat{\mathbf{g}}_k - \mathbf{g}_k\|_2 \leq 2\sqrt{2\tau\sigma H}$$

with probability at least  $1 - (s/d)^{O(s)}$ .

In Appendix C we quantify precisely how large  $n$  should be. Let us combine this with the estimates of Theorem 4.1.

**Corollary 5.6.** Assume the hypotheses of Theorem 5.5. Let  $r(x) = 0$  and let  $x_K$  be the iterate returned by ZORO with  $\alpha < 2/L$  after making  $T$  oracle queries, where  $K = T/m$ . Then:

1. If  $f(x)$  is convex, coercive and  $\|\nabla f(x)\|_2$  is coercive with respect to  $f(x)$ :

$$\begin{aligned} e_K &\leq \max \left\{ \frac{c_3 e_0 R^2}{T e_0 / c_1 s \log(d/s) + 2c_3 R^2}, 2^{\frac{3}{4}} R c_4^{\frac{1}{2}} (\tau\sigma H)^{\frac{1}{4}} \right\} \\ &= O \left( \max \left\{ \frac{s \log(d/s)}{T}, R(\sigma H)^{\frac{1}{4}} \right\} \right). \end{aligned}$$

with probability  $1 - (s/d)^{O(s)}$ .

2. If  $f(x)$  is convex and restricted  $\nu$ -strongly convex:

$$e_K \leq c_6^{T/c_1 s \log(d/s)} + 2^{3/2} (1 - c_6)^{-1} c_7 (\tau\sigma H)^{1/2}.$$

again with probability  $1 - (s/d)^{O(s)}$ .

Finally, we consider the noisy oracle, regularized case.

**Corollary 5.7.** Let  $F(x) = f(x) + r(x)$  with  $f(x)$  convex and satisfying Assumptions 1.a, 2 and 3 and  $r(x)$  a closed proper convex function. Choose  $\alpha = 1/L$  and let  $\{x_1, \dots, x_K\}$  be the iterates found by ZORO after making  $T$  total oracle queries, where  $K = T/m$ . Then:

$$\min_{i=1, \dots, K} F(x_i) - \min F \leq \frac{s \log(d/s) R}{2T} + 2\sqrt{2\tau\sigma H},$$

with probability at least  $1 - (s/d)^{O(s)}$ .

### 5.3 Fixed gradient support

As a final example, we consider the case where  $\text{supp}(\nabla f(x)) = S$  for all  $x \in \mathbb{R}^d$ . We consider ZORO with Algorithm 4.

**Theorem 5.8.** *Suppose that  $f(x)$  is convex, coercive and satisfies Assumption 1.a. Suppose that  $r(x) = 0$  and  $\sigma = 0$ . Choose  $\alpha < 1/L$  and  $\varepsilon_{\text{rel}} < \min \left\{ \frac{1-\alpha L}{2-\alpha L}, \frac{2-\alpha L}{4-\alpha L}, \min_{i:i \in S} |(g_0)_i| / \|g_0\|_2 \right\}$  and define:*

$$\beta = \varepsilon_{\text{rel}} \left( \frac{1 - \alpha L - \varepsilon_{\text{rel}}(2 - \alpha L)}{1 - \varepsilon_{\text{rel}}} \right) \frac{2\varepsilon_{\text{inv}}}{sH}$$

*Suppose that  $\|g_0 - \hat{g}_0\|_2 \leq \varepsilon_{\text{rel}}\|g_0\|_2$ . For  $k = 1, \dots, K$ , choose OppGradEst (Algorithm 4) in line 7 of ZORO (Algorithm 1) with  $\phi > 0$ , and let  $x_K$  be the iterate found by ZORO after making  $T$  oracle queries, where  $K = T/s$ . Then:*

$$e_K \leq \frac{c_5 e_0 R^2}{T e_0 / c_1 s + c_5 R^2} = O\left(\frac{s}{T}\right)$$

*with probability at least  $1 - O(\varepsilon_{\text{inv}})$ .*

Theorem 5.8 is rather optimistic; in particular, it would be hard to guarantee  $\varepsilon_{\text{rel}}$  satisfies the required condition in practice. Nevertheless, it gives some indication of the best possible performance of ZORO with opportunistic gradient estimation. In reality, we expect the performance to be somewhere between this and the more pessimistic guarantees of Sections 5.1 and 5.2. We note that Theorem 5.8 requires  $\|g_0 - \hat{g}_0\|_2 \leq \varepsilon_{\text{rel}}\|g_0\|_2$ . In Appendix C, we discuss how to do this without making too many more queries.

## 6 Numerical experiments

In this section, we demonstrate the practical usefulness of our method and compare its performance with other gradient estimation methods. There have been considerable efforts on zeroth-order *global* optimization methods for high dimensional problems, *e.g.*, REMBO (Wang et al., 2013). In this paper, we will not compare the performances between any global and ZORO directly, due to their strong correlations with problem structures. Furthermore, for the fairness of the comparison, we only use Algorithm 3 for CoSaMP gradient estimations in this section, so ZORO does not gain extra advantage from the consistent gradient supports with opportunistic gradient estimation.

### 6.1 Synthetic example

We consider the problem of minimizing a quadratic function  $f(x) = x^\top A x / 2$ , where  $A \in \mathbb{R}^{200 \times 200}$  is a diagonal matrix. We experiment two cases: (a) exact sparse case where only 20 diagonal elements are non-zero randomly generated positive numbers; (b) approximately sparse case where all diagonal elements are non-zero but the diagonal element values diminish exponentially with respect to the row/column indexes, *i.e.*,  $A_{i,i} = e^{-\omega i}$  with  $\omega > 0$ .

In case (a), for CoSaMP and OMP, we use the sparsity level and number of samples according to the sparse structure of the objective function. We use the same number of samples for LASSO. We use an identical step size for all methods except SPSSA, whose convergence is not robust with large step size in practice. We also tested a proximal operator to enforce non-negative values. The

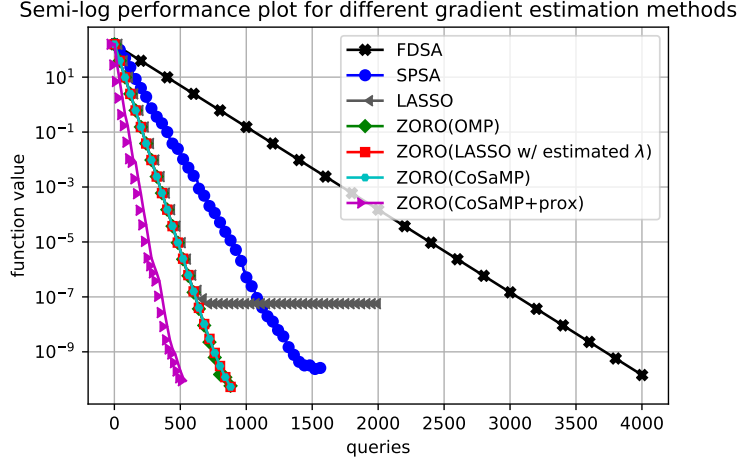


Figure 1: Function values *v.s.* queries comparisons between gradient estimation methods: exact sparse case.

results are shown in Figure 1. Unsurprisingly, FDSA-based approach has the slowest convergence rate because it over-samples in the redundant dimensions. CoSaMP with proximal operator only requires about 50% total queries compared to other sparse coding methods without any proximal operator.

Note that if we use a fixed regularizing parameter  $\lambda$  for LASSO, then the function would often saturate at large iterations. The reason is that the ratio between the  $\ell_2$ -norm square term and the  $\ell_1$  term becomes too small to recover any non-zero gradient. To address this issue, we propose a numerical rule for estimating the regularizing parameter of LASSO. At iteration  $k + 1$ , we use the  $\ell_2$ -norm square and  $\ell_1$  terms from the last iteration to estimate the new parameter:  $\lambda_{k+1} = c \|\mathbf{y}_k - Z_k \hat{\mathbf{g}}_k\|_2^2 / \|\hat{\mathbf{g}}_k\|_1$ , where  $c$  is a fixed parameter throughout the optimisation,  $\mathbf{y}_k$  is the vector of function differences,  $Z_k$  is the perturbation matrix, and  $\hat{\mathbf{g}}_k$  is the previous estimated gradient. With this one-tap delay trick, LASSO converges at the same speed as other sparse gradient estimation methods, in terms of query complexity.

We further investigate the running time differences among three sparse coding methods, by recording 30 iterations of gradient descent. We compare their speeds under different dimensions and sparsity levels, which are summarized as Figures 5 and 6 in Appendix D. We find the greedy methods, CoSaMP and OMP, have speed advantage when the problem dimension  $d$  is large and sparsity level  $s$  is small, while LASSO solvers win the speed in the case of both  $d$  and  $s$  are mild. We emphasize that the gradients estimated by these three methods offer almost identical convergence performance on the easier synthetic tasks, so stop criteria will not affect our observation in this experiment.

We now discuss case (b), where we use a decay factor  $\omega = 0.5$ . The main challenge here is that the approximate sparsity level changes (mostly grows) over iterations. We add the simulation of the adaptive strategy described in Section 3.2 to handle this issue. We include the simulation of applying the adaptive strategy and the proximal operator, which converges the fastest among all methods. To demonstrate the effect of adaptive strategy, we plot the sparsity levels used at

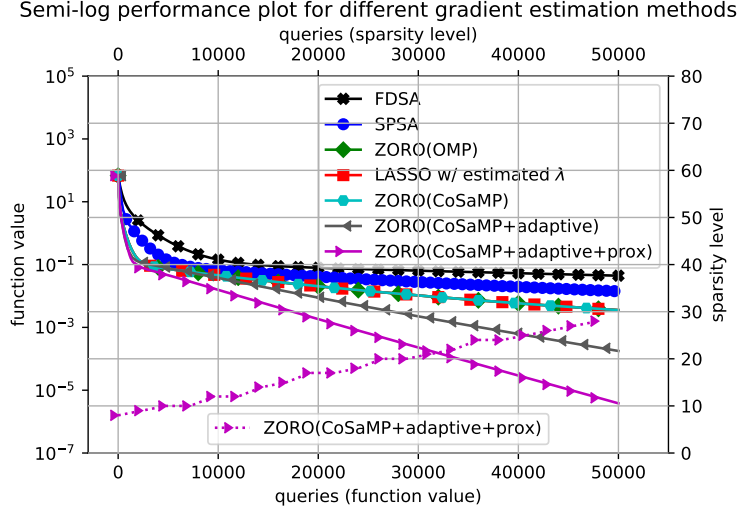


Figure 2: Function values *v.s.* queries comparisons between gradient estimation methods: approximately sparse case.

different iterations. All the simulation results are shown in Figure 2.

## 6.2 Asset risk management

We consider risk minimization problem for asset management. Suppose that a portfolio consists of  $n$  different assets. The rate of return of asset  $i$  is a random variable with expected value  $m_i$ . We use  $\mathcal{C}$  to denote the covariance matrix of asset returns. The portfolio risk, which we aim to minimize, can be written as  $\frac{x^\top \mathcal{C} x}{2(\sum_{i=1}^n x_i)^2}$ . Specifically for our experiments, we use the correlation, mean, and standard deviation of 225 assets from the dataset of (Chang et al., 2000). Our goal is to minimize the risk function given that the expected return should be no less than a minimal rate of portfolio return that the investor desires.  $\frac{\sum_{i=1}^n m_i x_i}{\sum_{i=1}^n x_i} > r$ . We include a penalty term to the risk function to describe the minimal rate return constraint and formulate the problem as follows:

$$\underset{x \in \mathbb{R}^d}{\text{minimize}} \frac{x^\top \mathcal{C} x}{2(\sum_{i=1}^n x_i)^2} + \lambda \left( \min \left\{ \frac{\sum_{i=1}^n m_i x_i}{\sum_{i=1}^n x_i} - r, 0 \right\} \right)^2.$$

If the optimizer has access to all the parameters, then it is natural to use quadratic programming methods to minimize the risk function. We are interested in cases where the optimizer can only access the objective function values. A natural benefit of such setting is that the optimizer has no access to the model or associated data and provides service in a “federated” fashion (*e.g.*, SigOPT).

We first experiment the case where no constraints are applied on the allocation vector, *i.e.*,  $x_i$  can be negative. In other words, for each asset, the final solution can be either long or short-sell. We use fixed sparsity level and sample numbers in this experiment. We use an identical randomly-generated initial point for all experiments. We have tuned the parameters for different sparse recovery methods to achieve their best convergence speed, respectively. The results are shown in

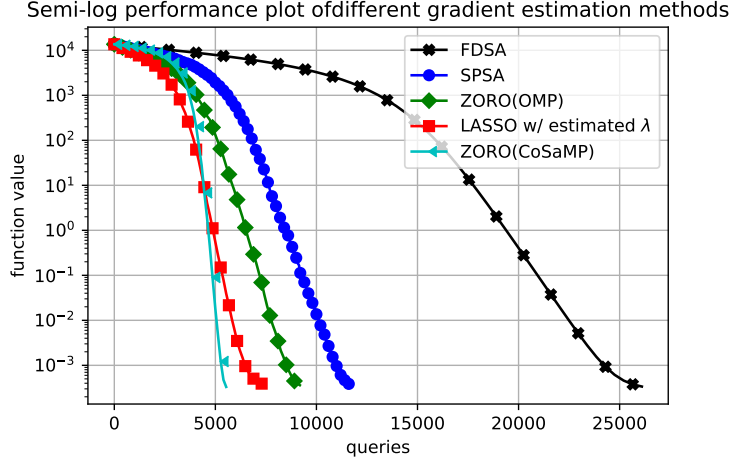


Figure 3: Function values *v.s.* queries comparisons between gradient estimation methods.

Figure 3. Note that CoSaMP has the best convergence rate among all methods. The final risks of all the methods are approximately  $2 \times 10^{-4}$ , which is consistent with the optimal risk using quadratic programming.

We now consider the long-only solution, *i.e.*,  $x_i \geq 0$  for all  $i$ . To handle the constraints, we apply the following proximal operators after each gradient descent iteration:

$$x_i = x_i + |\min\{0, \min_{j=1, \dots, n} x_j\}|, \quad \forall i,$$

$$x_i = x_i / \sum_{j=1}^n x_j, \quad \forall i.$$

The first update shifts the variables based on the smallest negative variable (if any) to satisfy the long-only constraint. The second update projects an allocation in amount to an allocation in fractions. Here We implemented the adaptive strategy for CoSaMP and OMP. The results are shown in Figure 4. Note that for SPSA, we are unable to obtain a set of parameters for stable convergence; partially due to the sensitivity to the step size along with proximal operator. FDSA method converges to the optimum but is the least query-efficient. Gradient estimate methods with LASSO, OMP, and CoSaMP converge using carefully tuned hyper-parameters. We also find that the step size for CoSaMP gradient update can be more aggressive than those of LASSO and OMP, which leads to its out-performance. Comparing with the non-regularized case, the query complexities are significantly reduced for all methods with proximal operator and adaptive strategy.

### 6.3 Sparse adversarial attack on ImageNet

We consider the problem of generating black-box adversarial examples using zeroth-order optimization methods. We use Inception-V3 model (Szegedy et al., 2016) on ImageNet (Deng et al., 2009) and focus on per-image adversarial attack problem. The authors in (Chen et al., 2019) considered a similar problem by optimizing the attack loss and the  $\ell_2$ -norm of image distortion. In contrast,



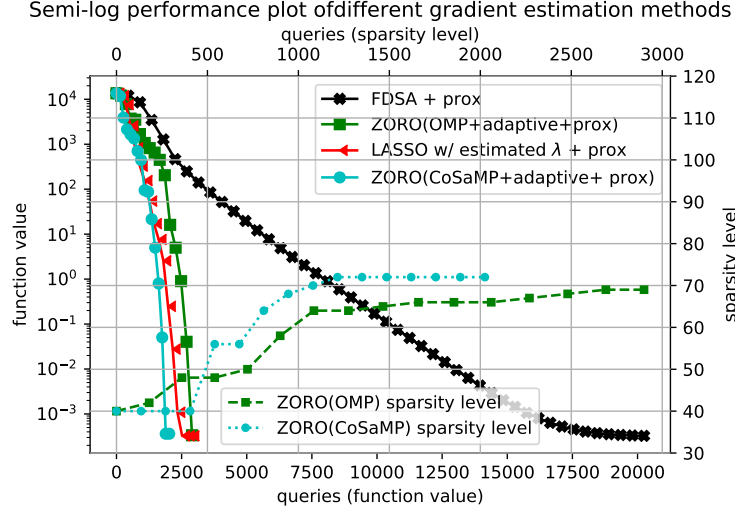


Figure 4: Function values *v.s.* queries comparisons between gradient estimation methods.

we aim to design a distortion  $\delta$  for a single image  $x$  such that the attack loss  $f(x + \delta)$  and the  $\ell_0$  norm of distortion are minimized:  $\text{minimize}_{\delta} f(x + \delta) + \lambda \|\delta\|_0$ . Note that all the methods in (Chen et al., 2019) lead to extremely large  $\ell_0$  distortion norm, except ZO-SCD, which has the worse  $\ell_2$  distortion norm. In other words, the successful attacks require distorting at (almost) all pixels. We compare ZORO with ZO-AdaMM, ZO-SGD, and ZO-SCD (Chen et al., 2019). Note that ZO-SCD is essentially a variation of FDSA and ZO-SGD is a mini-batched version of SPSA. For these methods, we use the same experiment setup from (Chen et al., 2019), which uses 10 queries at each iteration and determines if the attack successes before 1000 iterations. For ZORO, we generate 50 queries at each iteration for sparse recovery and determine if attack successes before 200 iterations. At each iteration of sparse recovery, we randomly select a subspace of 2000 dimensions (pixels) and generate random perturbations only in this subspace. We note that sparse adversarial attacks have been investigated before, *e.g.*, SparseFool (Modas et al., 2019). To the best of our knowledge, we are the first to connect adversarial attack to sparse coding based zeroth-order optimization.

We present the detailed experiment results in Table 1. Note that the attack success rate of ZORO is best among all methods. The average distortion  $\ell_0$  loss is smaller than ZO-SCD. Surprisingly, the average distortion  $\ell_2$  loss of ZORO attacks is also the best among all zeroth-order methods. Note that the average iterations of ZORO is the best among all methods, but the average query is the worst since it uses more queries at each iteration.

We apply a median filter to attempt mitigating the adversarial attack. We use Inception-V3 on filtered image to check if the model identifies the true label. We apply the same filter to the original image and check if the median filter itself damages the model. We summarize the total reduction in prediction accuracy on the set of adversarial and original images due to the mitigated adversarial attacks and the distortion from median filter. The results are shown in Table 2. We note that with a median filter, there is a good chance that the attacks can be mitigated. The catch is that the median filter could also potentially distorted the original images to fool the model.

Table 1: Attack successful rate (ASR), average final  $\ell_0$  distortion (as a percentage of total pixel numbers), average final  $\ell_2$  distortion, and average iterations of 1st successful attack for different zeroth-order attack methods.

METHODS	ASR	$\ell_0$ DIST	$\ell_2$ DIST	ITER
ZO-SCD	78 %	0.89%	57.5	240
ZO-SGD	78%	100%	37.9	159
ZO-AdaMM	81%	100%	28.2	172
ZORO	<b>90%</b>	<b>0.73%</b>	<b>21.1</b>	<b>59</b>

Table 2: Recover successful rate (RSR), original image distortion rate, and total prediction accuracy reduction for different median filter sizes.

MEDIAN FILTER	RSR	DIST RATE	TOT REDUCTION
size = 2	86 %	8%	21%
size = 3	<b>92</b> %	<b>7</b> %	<b>14</b> %
size = 4	76 %	14%	34%
size = 5	69 %	29%	53%

## Acknowledgments

The work of the first two authors was partially supported by NSF Grant DMS-1720237 and ONR Grant N000141712162. The authors would like to thank Drs. Rong Jin and Jian Tan for helpful discussions.

## References

- Agarwal, A., Dekel, O., and Xiao, L. Optimal algorithms for online convex optimization with multi-point bandit feedback. In *COLT*, pp. 28–40. Citeseer, 2010.
- Balasubramanian, K. and Ghadimi, S. Zeroth-order (non)-convex stochastic optimization via conditional gradient and gradient updates. In *Advances in Neural Information Processing Systems*, pp. 3455–3464, 2018.
- Baraniuk, R., Davenport, M., DeVore, R., and Wakin, M. A simple proof of the restricted isometry property for random matrices. *Constructive Approximation*, 28(3):253–263, 2008.
- Chang, T.-J., Meade, N., Beasley, J. E., and Sharaiha, Y. M. Heuristics for cardinality constrained portfolio optimisation. *Computers & Operations Research*, 27(13):1271–1302, 2000.
- Chen, X., Liu, S., Xu, K., Li, X., Lin, X., Hong, M., and Cox, D. Zo-adamm: Zeroth-order adaptive momentum method for black-box optimization. In *Advances in Neural Information Processing Systems*, pp. 7202–7213, 2019.
- Choromanski, K., Rowland, M., Sindhvani, V., Turner, R. E., and Weller, A. Structured evolution with compact architectures for scalable policy optimization. *arXiv preprint arXiv:1804.02395*, 2018.
- Deng, J., Dong, W., Socher, R., Li, L.-J., Li, K., and Fei-Fei, L. Imagenet: A large-scale hierarchical image database. In *2009 IEEE conference on computer vision and pattern recognition*, pp. 248–255. Ieee, 2009.
- Duchi, J. C., Jordan, M. I., Wainwright, M. J., and Wibisono, A. Optimal rates for zero-order convex optimization: The power of two function evaluations. *IEEE Transactions on Information Theory*, 61(5):2788–2806, 2015.
- Fan, J. and Li, R. Variable selection via nonconcave penalized likelihood and its oracle properties. *Journal of the American statistical Association*, 96(456):1348–1360, 2001.
- Flaxman, A. D., Kalai, A. T., and McMahan, H. B. Online convex optimization in the bandit setting: gradient descent without a gradient. *arXiv preprint cs/0408007*, 2004.
- Foucart, S. Sparse recovery algorithms: sufficient conditions in terms of restricted isometry constants. In *Approximation Theory XIII: San Antonio 2010*, pp. 65–77. Springer, 2012.
- Ghadimi, S. and Lan, G. Stochastic first-and zeroth-order methods for nonconvex stochastic programming. *SIAM Journal on Optimization*, 23(4):2341–2368, 2013.
- Gu, B., Huo, Z., Deng, C., and Huang, H. Faster derivative-free stochastic algorithm for shared memory machines. In *International Conference on Machine Learning*, pp. 1812–1821, 2018.
- Jamieson, K. G., Nowak, R., and Recht, B. Query complexity of derivative-free optimization. In *Advances in Neural Information Processing Systems*, pp. 2672–2680, 2012.
- Kiefer, J., Wolfowitz, J., et al. Stochastic estimation of the maximum of a regression function. *The Annals of Mathematical Statistics*, 23(3):462–466, 1952.

- Kurakin, A., Goodfellow, I., and Bengio, S. Adversarial machine learning at scale. *arXiv preprint arXiv:1611.01236*, 2016.
- Larson, J., Menickelly, M., and Wild, S. M. Derivative-free optimization methods. *Acta Numerica*, 28:287–404, 2019.
- Lian, X., Zhang, H., Hsieh, C.-J., Huang, Y., and Liu, J. A comprehensive linear speedup analysis for asynchronous stochastic parallel optimization from zeroth-order to first-order. In *Advances in Neural Information Processing Systems*, pp. 3054–3062, 2016.
- Liu, S., Chen, J., Chen, P.-Y., and Hero, A. Zeroth-order online alternating direction method of multipliers: Convergence analysis and applications. In *International Conference on Artificial Intelligence and Statistics*, pp. 288–297, 2018.
- Liu, S., Chen, P. Y., Chen, X., and Hong, M. Signsgd via zeroth-order oracle. In *7th International Conference on Learning Representations, ICLR 2019*, 2019.
- Modas, A., Moosavi-Dezfooli, S.-M., and Frossard, P. Sparsefool: a few pixels make a big difference. In *Proceedings of the IEEE Conference on Computer Vision and Pattern Recognition*, pp. 9087–9096, 2019.
- Nakamura, N., Seepaul, J., Kadane, J. B., and Reeja-Jayan, B. Design for low-temperature microwave-assisted crystallization of ceramic thin films. *Applied Stochastic Models in Business and Industry*, 33(3):314–321, 2017.
- Needell, D. and Tropp, J. A. Cosamp: Iterative signal recovery from incomplete and inaccurate samples. *Applied and computational harmonic analysis*, 26(3):301–321, 2009.
- Nesterov, Y. and Spokoiny, V. Random gradient-free minimization of convex functions. *Technical report, Universite catholique de Louvain, Center for Operations Research and Econometrics (CORE)*, 2011.
- Nesterov, Y. and Spokoiny, V. Random gradient-free minimization of convex functions. *Foundations of Computational Mathematics*, 17(2):527–566, 2017.
- Papernot, N., McDaniel, P., Goodfellow, I., Jha, S., Celik, Z. B., and Swami, A. Practical black-box attacks against machine learning. In *Proceedings of the 2017 ACM on Asia conference on computer and communications security*, pp. 506–519, 2017.
- Schmidt, M., Roux, N. L., and Bach, F. R. Convergence rates of inexact proximal-gradient methods for convex optimization. In *Advances in neural information processing systems*, pp. 1458–1466, 2011.
- Schöpfer, F. Linear convergence of descent methods for the unconstrained minimization of restricted strongly convex functions. *SIAM Journal on Optimization*, 26(3):1883–1911, 2016.
- Shamir, O. On the complexity of bandit and derivative-free stochastic convex optimization. In *Conference on Learning Theory*, pp. 3–24, 2013.
- Snoek, J., Larochelle, H., and Adams, R. P. Practical bayesian optimization of machine learning algorithms. In *Advances in neural information processing systems*, pp. 2951–2959, 2012.

- Spall, J. C. An overview of the simultaneous perturbation method for efficient optimization. *Johns Hopkins apl technical digest*, 19(4):482–492, 1998.
- Szegedy, C., Vanhoucke, V., Ioffe, S., Shlens, J., and Wojna, Z. Rethinking the inception architecture for computer vision. In *Proceedings of the IEEE conference on computer vision and pattern recognition*, pp. 2818–2826, 2016.
- Taskar, B., Chatalbashev, V., Koller, D., and Guestrin, C. Learning structured prediction models: A large margin approach. In *Proceedings of the 22nd international conference on Machine learning*, pp. 896–903, 2005.
- Tikhomirov, K. Singularity of random bernoulli matrices. *Annals of Mathematics*, 191(2):593–634, 2020.
- Wang, Y., Du, S., Balakrishnan, S., and Singh, A. Stochastic zeroth-order optimization in high dimensions. In *International Conference on Artificial Intelligence and Statistics*, pp. 1356–1365, 2018.
- Wang, Z., Zoghi, M., Hutter, F., Matheson, D., and De Freitas, N. Bayesian optimization in high dimensions via random embeddings. In *Twenty-Third International Joint Conference on Artificial Intelligence*, 2013.
- Zhang, H. The restricted strong convexity revisited: analysis of equivalence to error bound and quadratic growth. *Optimization Letters*, 11(4):817–833, 2017.
- Zhang, H. and Cheng, L. Restricted strong convexity and its applications to convergence analysis of gradient-type methods in convex optimization. *Optimization Letters*, 9(5):961–979, 2015.

# ZORO: Supplemental Materials

In this supplementary material we provide the proofs for the main theorems presented in the main article and present the results of some additional numerical experiments. Specifically, in section A we present the proofs for Section 3 in the main article, which center around the accuracy of the gradient estimator used in ZORO. Section B contains several technical results on sequences and inexact gradient descent, and culminates in the proofs of Theorems 4.1 and 4.2. In section C we present the proofs of our main results, namely those contained in section 5, while in section D we present some additional numerical results that may be of interest.

Before proceeding, for the reader's convenience, we provide a table of notation here (see Table 3).

Table 3: Table of Notation.

NOTATION	DEFINITION
$d$	dimension of $x$
$f(x)$	underlying loss function
$s$	sparsity of $\nabla f$ (when it is sparse)
$r(x)$	regularization function
$F(x)$	$f(x) + r(x)$ , if $r$ is non-zero
$\min f$	$\min\{f(x) : x \in \mathbb{R}^d\}$ , minimum value of $f$
$e_k$	$f(x_k) - \min f$ , objective error
$x_k$	$k$ -th iterate of ZORO
$z_i$	Rademacher random variable, see (10)
$n$	number of iterations of CoSaMP in ZORO
$\mathbf{g}_k$	$\nabla f(x_k)$ , true gradient at $x_k$
$\hat{\mathbf{g}}_k$	estimated gradient at $x_k$
$\mathbf{e}_k$	$\hat{\mathbf{g}}_k - \mathbf{g}_k$ , gradient estimation error
$H$	uniform bound of $\ \nabla^2 f\ _1$ (Asm. 2)
$L$	Lipschitz constant of $\nabla f$ (Asm. 3)
$\nu$	restricted strong convexity of $f$ (Def. 2)
$E_f(x)$	oracle query of $f(x)$ , see (2)
$\xi$	oracle noise
$\sigma$	bound of $\xi$ (Asm. 4)
$m$	number of samples
$\delta$	sampling radius, see (11)
$\ \cdot\ _0$	$\ell_0$ -norm
$\ \cdot\ _1$	$\ell_1$ -norm
$\ \cdot\ _2$	$\ell_2$ -norm
$\ \cdot\ _\infty$	$\ell_\infty$ -norm
$[\cdot]_{(s)}$	best $s$ -sparse approximate
$\mathbf{P}_*(\cdot)$	projection onto the solution set
$\mathbb{P}[\cdot]$	probability
$\mathbb{E}[\cdot]$	expectation

## A Proofs for Section 3

*Proof of Lemma 3.1.* The proof is similar to the argument of Section 3 in (Wang et al., 2018), but we include it for completeness. From Taylor's theorem:

$$f(x + \delta z_i) = f(x) + \delta z_i^\top \mathbf{g} + \frac{\delta^2}{2} z_i^\top \nabla^2 f(x + tz_i) z_i$$

for some  $t \in (0, 1)$ . Assuming  $E_f(x + \delta z_i) = f(x + \delta z_i) + \xi_+$  and  $E_f(x) = f(x) + \xi_-$ , equation (11) becomes:

$$y_i = \frac{1}{\sqrt{m}} z_i^\top \mathbf{g} + \frac{\xi_+ - \xi_-}{\sqrt{m}} + \frac{\delta}{2\sqrt{m}} z_i^\top \nabla^2 f(x + tz_i) z_i.$$

Let  $\mu_i := \frac{\xi_+ - \xi_-}{\sqrt{m}}$ , then  $|\mu_i| \leq 2\sigma/\sqrt{m}$ . Let  $\nu_i = z_i^\top \nabla^2 f(x + tz_i) z_i / (2\sqrt{m})$ . Now:

$$\begin{aligned} 2\sqrt{m}|\nu_i| &= |z_i^\top \nabla^2 f(x + t_0 \delta z_i) z_i| \\ &= \left| \sum_{j,k} \nabla_{j,k}^2 f(x + t_0 \delta z_i) (z_i)_j (z_i)_k \right| \\ &\leq \|\nabla^2 f(x + t_0 \delta z_i)\|_1 \|z_i\|_\infty^2 \leq H \end{aligned}$$

by Assumption 2 and the fact that  $\|z_i\|_\infty = 1$ . □

For future use, let  $\boldsymbol{\mu} = [\mu_1, \dots, \mu_m]^\top$  and  $\boldsymbol{\nu} = [\nu_1, \dots, \nu_m]^\top$ . Then:

$$\mathbf{y} = Z\mathbf{g} + \frac{1}{\delta}\boldsymbol{\mu} + \delta\boldsymbol{\nu}. \quad (15)$$

### A.1 Proof of Theorem 3.2

For the convenience of the reader we begin by recalling a few theorems from the literature.

**Theorem A.1** (Theorem 5.2 of (Baraniuk et al., 2008)). *If  $m = c_1 s \log(d/s)$  then  $Z$  satisfies the Restricted Isometry Property (RIP) with constant  $\delta_{4s}(Z) \leq 0.3843$  with probability  $1 - (s/d)^{c_2 s}$ . Here  $c_1$  and  $c_2$  are constants independent of  $s, d$  and  $m$ .*

We remind the reader that  $Z$  has the  $(4s)$ -RIP if, for all  $\mathbf{v} \in \mathbb{R}^d$  with  $\|\mathbf{v}\|_0 \leq 4s$ :

$$(1 - \delta_{4s}(Z))\|\mathbf{v}\|_2^2 \leq \|Z\mathbf{v}\|_2^2 \leq (1 + \delta_{4s}(Z))\|\mathbf{v}\|_2^2.$$

The choice of the value 0.3843 is to match with the assumptions of (Foucart, 2012), which we state next. Recall that  $[\mathbf{g}]_{(s)}$  denotes the best  $s$ -sparse approximation to  $\mathbf{g}$ .

**Theorem A.2** (Theorem 5 of (Foucart, 2012)). *Let  $\{\mathbf{g}^n\}$  be the sequence generated by applying CoSaMP (Needell & Tropp, 2009) to problem (12), with  $m \geq c_1 s \log(d/s)$  and initialization  $\mathbf{g}^0 = \mathbf{0}$ . Then, with probability  $1 - (s/d)^{c_2 s}$ : for all  $\mathbf{g}$ ,*

$$\|\mathbf{g}^n - [\mathbf{g}]_{(s)}\|_2 \leq \tau \left\| Z(\mathbf{g} - [\mathbf{g}]_{(s)}) + \frac{1}{\delta}\boldsymbol{\mu} + \delta\boldsymbol{\nu} \right\|_2 + \rho^n \|\mathbf{g}\|_{(s)} \quad (16)$$

where  $\rho < 1$  and  $\tau \approx 10$  depend only on  $\delta_{4s}$ .

The exact values of  $\rho$  and  $\tau$  are provided in (Foucart, 2012). Note that the constants  $c_1, c_2$  are the same as in Theorem A.1. Certainly, other initializations are possible. For example, when using the ZORO method we have found that taking  $\mathbf{g}^0$  to be the gradient estimator found at the previous step, *i.e.*  $\mathbf{g}^0 = \hat{\mathbf{g}}_{k-1}$ , offers a modest speed-up.

**Theorem A.3** (Proposition 3.5 in (Needell & Tropp, 2009)). *Suppose that  $Z$  satisfies the  $(4s)$ -RIP. Then for any  $\mathbf{v} \in \mathbb{R}^d$ :*

$$\|Z\mathbf{v}\|_2 \leq \sqrt{1 + \delta_{4s}(Z)} \left( \|\mathbf{v}\|_2 + \frac{1}{\sqrt{s}} \|\mathbf{v}\|_1 \right)$$

**Theorem A.4** (Concentration of measure). *Suppose that  $Z = \frac{1}{\sqrt{m}}A \in \mathbb{R}^{m \times d}$  where:*

$$A_{ij} = \begin{cases} +1 & \text{with probability } 1/2 \\ -1 & \text{with probability } 1/2 \end{cases}$$

*Then for any  $\varepsilon > 0$  and any  $\mathbf{v} \in \mathbb{R}^d$ :*

$$\mathbb{P} \left[ \left| \|Z\mathbf{v}\|_2^2 - \|\mathbf{v}\|_2^2 \right| \geq \varepsilon \|\mathbf{v}\|_2^2 \right] \leq 2e^{-mc_0(\varepsilon)}$$

where  $c_0(\varepsilon) := \varepsilon^2/4 - \varepsilon^3/6$ .

*Proof.* See, for example, Section 4 of (Baraniuk et al., 2008) and references contained therein.  $\square$

Note that it follows from (16) that:

$$\|\mathbf{g}^n - \mathbf{g}\|_2 \leq \|\mathbf{g} - [\mathbf{g}]_{(s)}\|_2 + \tau \|Z(\mathbf{g} - [\mathbf{g}]_{(s)})\|_2 + \frac{\tau}{\delta} \|\boldsymbol{\mu}\|_2 + \tau \delta \|\boldsymbol{\nu}\|_2 + \rho^n \|\mathbf{g}\|_{(s)} \quad (17)$$

**Lemma A.5.** *Suppose that  $f$  satisfies Assumption 1.c. Then  $\|\mathbf{g} - [\mathbf{g}]_{(s)}\|_2 + \tau \|Z(\mathbf{g} - [\mathbf{g}]_{(s)})\|_2 \leq \psi \|\mathbf{g}\|_2$  where:*

$$\psi = \left( \left( 1 + \tau \sqrt{1 + \delta_{4s}(Z)} \right) \left( \frac{2}{p} - 1 \right)^{-1/2} + \tau \sqrt{1 + \delta_{4s}(Z)} \left( \frac{1}{p} - 1 \right)^{-1} \right) s^{1/2-1/p}$$

*Proof.* Combining the bounds (4),(5) and Theorem A.3 we obtain:

$$\begin{aligned} \|Z(\mathbf{g} - [\mathbf{g}]_{(s)})\|_2 &\leq \sqrt{1 + \delta_{4s}(Z)} \left( \|\mathbf{g} - [\mathbf{g}]_{(s)}\|_2 + \frac{1}{\sqrt{s}} \|\mathbf{g} - [\mathbf{g}]_{(s)}\|_1 \right) \\ &\leq \sqrt{1 + \delta_{4s}(Z)} \left( \left( \frac{2}{p} - 1 \right)^{-1/2} \|\mathbf{g}\|_2 s^{1/2-1/p} + \frac{1}{\sqrt{s}} \left( \frac{1}{p} - 1 \right)^{-1} \|\mathbf{g}\|_2 s^{1-1/p} \right) \\ &= \sqrt{1 + \delta_{4s}(Z)} \left( \left( \frac{2}{p} - 1 \right)^{-1/2} + \left( \frac{1}{p} - 1 \right)^{-1} \right) s^{1/2-1/p} \|\mathbf{g}\|_2 \end{aligned}$$

Use (5) again to bound  $\|\mathbf{g} - [\mathbf{g}]_{(s)}\|_2$  and add to obtain the lemma.  $\square$

**Lemma A.6.**  $\|\boldsymbol{\mu}\|_2 \leq 2\sigma$  and  $\|\boldsymbol{\nu}\|_2 \leq H/2$ .



*Proof.* From Lemma 3.1, we have

$$\|\boldsymbol{\mu}\|_2^2 = \sum_{i=1}^m \mu_i^2 \leq \sum_{i=1}^m \frac{4\sigma^2}{m} = 4\sigma^2.$$

Similarly, we also get

$$\|\boldsymbol{\nu}\|_2^2 = \sum_{i=1}^m \nu_i^2 \leq \sum_{i=1}^m \frac{H^2}{4m} = \frac{H^2}{4}.$$

□

Combining Lemmas A.5 and A.6 with equation (17), and using  $\|[\mathbf{g}]_{(s)}\|_2 \leq \|\mathbf{g}\|_2$ , yields Theorem 3.2.

## B Proofs for Section 4

We proceed via a series of Lemmas.

**Lemma B.1** (Sequence analysis). *Consider a sequence  $e_k \geq 0$  obeying  $e_{k+1} \leq e_k - ce_k^2 + d$  for  $k = 0, 1, \dots$  where  $c > 0$  and  $d \geq 0$ . We have*

$$e_k \leq \frac{e_0}{e_0 c \cdot k + 2}, \quad k \in \{t : e_0, \dots, e_{t+1} \geq \sqrt{2d/c}\}.$$

*In particular, if  $d = 0$ , then we get*

$$e_k \leq \frac{e_0}{e_0 c \cdot k + 1}, \quad k = 0, 1, \dots$$

The first result is a decay of  $e_k$  at rate  $\sim 1/(ck)$  up until  $e_k = \sqrt{2d/c}$ . The second result has the rate  $\sim 1/(ck)$  for all  $k$ .

*Proof.* Without loss of generality, assume  $e_k > 0$  for  $k = 0, 1, \dots$ . If  $e_k \geq \sqrt{2d/c}$ , then  $e_{k+1} \leq e_k - d$ , so  $\frac{e_k}{e_{k+1}} \geq 1$ . Dividing the condition by  $e_{k+1}e_k$  and reorganizing yields

$$\begin{aligned} \frac{1}{e_{k+1}} - \frac{1}{e_k} &\geq \frac{ce_k}{e_{k+1}} - \frac{d}{e_{k+1}e_k} \\ &\geq \begin{cases} c - \frac{d}{2d/c} = \frac{1}{2}c, & d \neq 0, \\ c, & d = 0. \end{cases} \end{aligned}$$

Summing, we obtain  $\frac{1}{e_k} \geq \frac{1}{e_0} + \frac{1}{2}kc$  when  $d \neq 0$  and  $\frac{1}{e_k} \geq \frac{1}{e_0} + kc$  when  $d = 0$ . Inverting both sides yields the claim. Note that we have assumed that  $e_{k+1} \geq \sqrt{2d/c}$  in the  $d \neq 0$  case. □

**Lemma B.2** (Sequence analysis). *Any nonnegative sequence  $e_k$  obeying  $ae_k \leq b(e_k - e_{k+1}) + c_k$  for  $b > a > 0$  and  $c_k \geq 0$  satisfies*

$$e_k \leq \frac{(b-a)^k e_0}{b^k} + \sum_{t=1}^k \frac{(b-a)^{t-1} c_{k-t}}{b^t}.$$

On the right-hand side, the first term presents geometric convergence at rate  $(b-a)/b$  and the second term is accumulated noise.

*Proof.* The condition gives us  $be_{k+1} \leq (b-a)e_k + c_k$  and thus  $e_{k+1} \leq \frac{b-a}{b}e_k + \frac{c_k}{b}$ . Repeatedly applying this inequality produces the result.  $\square$

The next lemma quantifies, under very general assumptions, the amount of descent per iteration we can expect from an inexact gradient descent.

**Lemma B.3.** *Suppose that  $f(x)$  satisfies Assumption 3. Then if  $x_{k+1} = x_k - \alpha \hat{\mathbf{g}}_k$ :*

$$f(x_{k+1}) \leq f(x_k) - \frac{c_0}{2} \|\alpha \hat{\mathbf{g}}_k\|_2^2 + \frac{1}{2c_0} \|\mathbf{g}_k - \hat{\mathbf{g}}_k\|_2^2 \quad (18)$$

$$f(x_{k+1}) \leq f(x_k) - \frac{c_0}{2} \|\alpha \mathbf{g}_k\|_2^2 + \frac{\alpha^2(c_0 + L)}{2} \|\mathbf{g}_k - \hat{\mathbf{g}}_k\|_2^2 \quad (19)$$

where  $c_0 = \frac{1}{\alpha} - \frac{L}{2}$

*Proof.* Define  $c_0 = \frac{1}{\alpha} - \frac{L}{2}$ . By  $x_{k+1} - x_k = -\alpha \hat{\mathbf{g}}_k$ ,

$$\begin{aligned} f(x_{k+1}) &\stackrel{(a)}{\leq} f(x_k) + \langle -\alpha \hat{\mathbf{g}}_k, \mathbf{g}_k \rangle + \frac{L}{2} \|\alpha \hat{\mathbf{g}}_k\|_2^2 \\ &= f(x_k) - \langle \alpha \hat{\mathbf{g}}_k, \hat{\mathbf{g}}_k \rangle - \langle \alpha \hat{\mathbf{g}}_k, \mathbf{g}_k - \hat{\mathbf{g}}_k \rangle + \frac{L}{2} \|\alpha \hat{\mathbf{g}}_k\|_2^2 \\ &\stackrel{(b)}{\leq} f(x_k) - c_0 \|\alpha \hat{\mathbf{g}}_k\|_2^2 + \frac{c_0}{2} \|\alpha \hat{\mathbf{g}}_k\|_2^2 + \frac{1}{2c_0} \|\mathbf{g}_k - \hat{\mathbf{g}}_k\|_2^2 \\ &= f(x_k) - \frac{c_0}{2} \|\alpha \hat{\mathbf{g}}_k\|_2^2 + \frac{1}{2c_0} \|\mathbf{g}_k - \hat{\mathbf{g}}_k\|_2^2, \end{aligned}$$

where (a) follows from Assumption 3 and (b) from applying Young's inequality to  $\langle -\alpha \hat{\mathbf{g}}_k, \mathbf{g}_k - \hat{\mathbf{g}}_k \rangle$  and merging its results with the terms  $\|\alpha \hat{\mathbf{g}}_k\|_2^2$  and  $\|\alpha \hat{\mathbf{g}}_k\|_2^2$ . By steps similar to (18),

$$\begin{aligned} f(x_{k+1}) &\leq f(x_k) + \langle -\alpha \hat{\mathbf{g}}_k, \mathbf{g}_k \rangle + \frac{L}{2} \|\alpha \hat{\mathbf{g}}_k\|_2^2 \\ &= f(x_k) - \langle \alpha \mathbf{g}_k, \mathbf{g}_k \rangle - \alpha \langle \hat{\mathbf{g}}_k - \mathbf{g}_k, \mathbf{g}_k \rangle \\ &\quad + \frac{L}{2} \|\alpha \mathbf{g}_k + \alpha \hat{\mathbf{g}}_k - \alpha \mathbf{g}_k\|_2^2 \\ &= f(x_k) - c_0 \|\alpha \mathbf{g}_k\|_2^2 - \alpha^2 c_0 \langle \hat{\mathbf{g}}_k - \mathbf{g}_k, \mathbf{g}_k \rangle \\ &\quad + \alpha^2 \frac{L}{2} \|\mathbf{g}_k - \hat{\mathbf{g}}_k\|_2^2 \\ &\leq f(x_k) - \frac{c_0}{2} \|\alpha \mathbf{g}_k\|_2^2 + \frac{\alpha^2(c_0 + L)}{2} \|\mathbf{g}_k - \hat{\mathbf{g}}_k\|_2^2. \end{aligned}$$

$\square$

Note that an immediate consequence of this lemma is the following:

**Lemma B.4.** Suppose that  $f(x)$  satisfies Assumption 3 and  $x_{k+1} = x_k - \alpha \hat{\mathbf{g}}_k$ . Then:

$$\begin{aligned} \sum_{t=0}^k \|\alpha \hat{\mathbf{g}}_t\|_2^2 &\leq c_1(f(x_0) - \min f) + c_2 \sum_{t=0}^k \|\hat{\mathbf{g}}_t - \mathbf{g}_t\|_2^2 \\ \sum_{t=0}^k \|\alpha \mathbf{g}_t\|_2^2 &\leq c_1(f(x_0) - \min f) + c'_2 \sum_{t=0}^k \|\hat{\mathbf{g}}_t - \mathbf{g}_t\|_2^2 \end{aligned}$$

for  $c_1 = \frac{4\alpha}{2-\alpha L}$ ,  $c_2 = \frac{4\alpha^2}{(2-\alpha L)^2}$ , and  $c'_2 = \frac{\alpha^2(2+\alpha L)}{2-\alpha L}$ .

*Proof.* Take the telescopic sums of (18) and (19) respectively.  $\square$

The next lemma prepares the conditions for us to apply Lemma B.1. Recall that  $P_*(\cdot)$  is a projection operator onto the solution set.

**Lemma B.5.** Suppose that  $f(x)$  is convex and satisfies Assumption 3. Then:

$$e_k^2 \leq c_3 \|x_k - P_*(x_k)\|_2^2 (e_k - e_{k+1}) + c_4 \|x_k - P_*(x_k)\|_2^2 \|\mathbf{g}_k - \hat{\mathbf{g}}_k\|_2^2 \quad (20)$$

for  $c_3 = \frac{4\alpha}{2-\alpha L}$  and  $c_4 = \frac{\alpha^2(2+\alpha L)}{2-\alpha L}$ . In addition, if  $\|\mathbf{g}_k - \hat{\mathbf{g}}_k\| \leq \varepsilon_{\text{rel}} \|\mathbf{g}_k\|$ , then

$$e_k^2 \leq c_5 \|x_k - P_*(x_k)\|_2^2 (e_k - e_{k+1}) \quad (21)$$

for  $c_5 = \frac{4\alpha}{2-\alpha L - \alpha^2 \varepsilon_{\text{rel}}^2 (2+\alpha L)}$ .

*Proof.* By existence of  $P_*(x_k)$  and convexity of  $f$ ,

$$\begin{aligned} e_k &= f(x_k) - f(P_*(x_k)) \leq \langle \mathbf{g}_k, x_k - P_*(x_k) \rangle \\ &\leq \|\mathbf{g}_k\|_2 \|x_k - P_*(x_k)\|_2 \end{aligned} \quad (22)$$

and thus  $e_k^2 \leq \|x_k - P_*(x_k)\|_2^2 \|\mathbf{g}_k\|_2^2$ . It remains to bound  $\|\mathbf{g}_k\|_2^2$ . By (19),

$$\frac{c_0}{2} \|\mathbf{g}_k\|_2^2 \leq e_k - e_{k+1} + \frac{\alpha^2(c_0 + L)}{2} \|\mathbf{g}_k - \hat{\mathbf{g}}_k\|_2^2,$$

and from this, when  $\|\mathbf{g}_k - \hat{\mathbf{g}}_k\|_2 \leq \varepsilon_{\text{rel}} \|\mathbf{g}_k\|_2$ , we further have

$$\frac{1}{2} (c_0 - \alpha^2 \varepsilon_{\text{rel}}^2 (c_0 + L)) \|\mathbf{g}_k\|_2^2 \leq e_k - e_{k+1},$$

where  $c_0 = \frac{1}{\alpha} - \frac{L}{2}$ . The proof completes after we substitute  $e_k^2 \leq \|x_k - P_*(x_k)\|_2^2 \|\mathbf{g}_k\|_2^2$  into the last two inequalities above to eliminate  $\|\mathbf{g}_k\|_2^2$ .  $\square$

Finally we need an important boundedness result. For notational convenience, define  $\mathbf{e}_k := \hat{\mathbf{g}}_k - \mathbf{g}_k$ .

**Theorem B.6.** Assume that  $f(x)$  is coercive, convex and satisfies Assumption 3.

1. If  $\|\mathbf{e}_k\|_2 \leq \varepsilon_{\text{rel}} \|\mathbf{g}_k\|_2$ ,  $\alpha < 2/L$  and  $\varepsilon_{\text{rel}} \leq (2 - L\alpha)/(4 - L\alpha)$  then there exists an  $R$  such that  $\|x_k - P_*(x_k)\|_2 \leq R$  for all  $k$ .

2. If in addition  $\|\nabla f(x)\|_2$  is coercive with respect to  $f(x)$  and  $\|\mathbf{e}_k\|_2 \leq \varepsilon_{\text{abs}}$  then there exists an  $R$  such that  $\|x_k - \mathbf{P}_*(x_k)\|_2 \leq R$ .

*Proof.* By rearranging (18), we obtain:

$$f(x_k) - f(x_{k+1}) \geq \frac{c_0}{2} \|\alpha \hat{\mathbf{g}}_k\|_2^2 - \frac{1}{2c_0} \|\mathbf{e}_k\|_2^2 \quad (23)$$

and similarly from (19):

$$f(x_k) - f(x_{k+1}) \geq \frac{c_0}{2} \|\alpha \mathbf{g}_k\|_2^2 - \frac{\alpha^2(c_0 + L)}{2} \|\mathbf{e}_k\|_2^2 \quad (24)$$

**Case 1:**  $\|\mathbf{e}_k\|_2 \leq \varepsilon_{\text{rel}} \|\mathbf{g}_k\|_2$  Under this assumption, one can easily show that:

$$\|\mathbf{e}_k\|_2 \leq \frac{\varepsilon_{\text{rel}}}{1 - \varepsilon_{\text{rel}}} \|\hat{\mathbf{g}}_k\|_2.$$

Because  $\hat{\mathbf{g}}_k = \frac{1}{\alpha}(x_k - x_{k+1})$  from (23) we get:

$$\begin{aligned} & f(x_k) - f(x_{k+1}) \\ & \geq \left( \frac{c_0}{2} - \frac{\varepsilon_{\text{rel}}^2}{2\alpha^2 c_0 (1 - \varepsilon_{\text{rel}})^2} \right) \|x_k - x_{k+1}\|_2^2 \end{aligned}$$

Recalling that  $c_0 = \frac{1}{\alpha} - \frac{L}{2}$  we see that for  $\alpha < 2/L$  and  $\varepsilon_{\text{rel}} \leq (2 - L\alpha)/(4 - L\alpha)$  the sequence  $\{f(x_k)\}$  is monotonically decreasing. By coercivity, there exists an  $R$  such that  $\|x_k - \mathbf{P}_*(x_k)\|_2 \leq R$  for all  $k$ .

**Case 2:**  $\|\mathbf{e}_k\|_2 \leq \varepsilon_{\text{abs}}$  Below we first show  $f(x^k)$  is uniformly bounded and then show  $\|x^k\|_2$  is so, too.

By the coercivity of  $\|\nabla f(x)\|_2$  with respect to  $f(x)$ . There exists an  $R_1$  such that whenever  $f(x) \geq R_1$ ,  $\|\nabla f(x)\|_2^2 \geq \frac{(c_0 + L)\varepsilon_{\text{abs}}}{c_0}$ . From (24) we obtain:

$$f(x_k) - f(x_{k+1}) \geq \frac{c_0 \alpha^2}{2} \|\mathbf{g}_k\|_2^2 - \frac{\alpha^2(c_0 + L)\varepsilon_{\text{abs}}}{2}.$$

So, when  $\|\mathbf{g}_k\|_2^2 \geq \frac{(c_0 + L)\varepsilon_{\text{abs}}}{c_0}$ ,  $f(x_{k+1}) \leq f(x_k)$ ; hence, whenever  $f(x_k) \geq R_1$ , the next iterate does not increase  $f$ . The first  $k > 0$  that gives  $f(x_k) \geq R_1$ , if it exists, must also give  $f(x_{k-1}) < R_1$  and thus  $f(x_k) \leq f(x_{k-1}) - \frac{c_0 \alpha^2}{2} \|\mathbf{g}_{k-1}\|_2^2 + \frac{\alpha^2(c_0 + L)\varepsilon_{\text{abs}}}{2} < R_2$  for  $R_2 = R_1 + \frac{\alpha^2(c_0 + L)\varepsilon_{\text{abs}}}{2}$ . Therefore,  $f(x_k) \leq \max\{R_2, f(x_0)\}$  uniformly. By the coercivity of  $f(x)$  with respect to  $\|x\|_2$ , there exists  $R$  such that  $\|x_k\|_2 \leq R$  uniformly as, otherwise, the sequence  $(f(x_k))$  is unbounded.  $\square$

*Proof of Theorem 4.1.* Rearranging (20) to fit the hypothesis of Lemma B.1 we get:

$$e_{k+1} \leq e_k - \frac{1}{c_3 R^2} e_k^2 + \frac{c_4}{c_3} \varepsilon_{\text{abs}}$$

where we are using the assumption  $\|x_k - \mathbf{P}_*(x_k)\|_2 \leq R$  as well as the fact that  $\|\mathbf{g}_k - \hat{\mathbf{g}}_k\|_2 \leq \varepsilon_{\text{abs}}$ . Applying Lemma B.1 yields the Part 1.

Rearranging (21) to fit the hypothesis of Lemma B.1, with  $d = 0$ , we get:

$$e_k^2 \leq c_5 R^2 (e_k - e_{k+1})$$

where again we have used  $\|x_k - P_*(x_k)\|_2 \leq R$ . Applying Lemma B.1 again proves Part 2.  $\square$

*Proof of Theorem 4.2.* Substituting (8) into the results of Lemma B.5 and dividing by a factor of  $e_k$  results in

$$\nu e_k \leq c_3 (e_k - e_{k+1}) + c_4 \|\mathbf{g}_k - \hat{\mathbf{g}}_k\|_2^2,$$

and if  $\|\mathbf{g}_k - \hat{\mathbf{g}}_k\|_2 \leq \varepsilon_{\text{rel}} \|\mathbf{g}_k\|_2$ ,

$$\nu e_k \leq c_5 (e_k - e_{k+1}).$$

The claims then directly follow from Lemma B.2. In particular, when  $\|\mathbf{g}_k - \hat{\mathbf{g}}_k\|_2^2 \leq \varepsilon_{\text{abs}}$  for all  $k$ , we have  $\sum_{t=1}^{\infty} c_6^{t-1} c_7 \|\mathbf{g}_k - \hat{\mathbf{g}}_k\|_2^2 \leq (1 - c_6)^{-1} c_7 \varepsilon_{\text{abs}}$ .  $\square$

## C Proofs for Section 5

*Proof of Theorem 5.1.* Applying Theorem 3.2 with  $\sigma = 0$  yields

$$\begin{aligned} \|\mathbf{g}_k - \hat{\mathbf{g}}_k\|_2 &\leq \frac{\tau \delta_k H}{2} + (\psi + \rho^n) \|\mathbf{g}_k\|_2 \\ &= \left( \frac{\tau \delta_k H}{2(\varepsilon_{\text{rel}} - \psi - \rho^n) \|\mathbf{g}_k\|_2} \right) (\varepsilon_{\text{rel}} - \psi - \rho^n) \|\mathbf{g}_k\|_2 + (\psi + \rho^n) \|\mathbf{g}_k\|_2, \end{aligned}$$

for all  $k$  with probability  $1 - (s/d)^{O(s)}$ . Now, to guarantee that  $\|\mathbf{g}_k - \hat{\mathbf{g}}_k\|_2 \leq \varepsilon_{\text{rel}} \|\mathbf{g}_k\|_2$  we need to choose

$$\delta_k \leq \frac{2(\varepsilon_{\text{rel}} - \psi - \rho^n) \|\mathbf{g}_k\|_2}{\tau H}. \quad (25)$$

Of course, we do not have access to  $\|\mathbf{g}_k\|_2$  when choosing  $\delta_k$ ; hence, we use  $\|\hat{\mathbf{g}}_{k-1}\|_2$  as a proxy. We use the inductive assumption that  $\|\mathbf{g}_{k-1} - \hat{\mathbf{g}}_{k-1}\|_2 \leq \varepsilon_{\text{rel}} \|\mathbf{g}_{k-1}\|_2$ , in which case we have that:

$$\begin{aligned} \|\hat{\mathbf{g}}_{k-1}\|_2 &= \|\hat{\mathbf{g}}_{k-1} - \mathbf{g}_{k-1} + \mathbf{g}_{k-1} - \mathbf{g}_k + \mathbf{g}_k\|_2 \\ &\leq \|\hat{\mathbf{g}}_{k-1} - \mathbf{g}_{k-1}\|_2 + \|\mathbf{g}_{k-1} - \mathbf{g}_k\|_2 + \|\mathbf{g}_k\|_2 \\ &\leq \varepsilon_{\text{rel}} \|\mathbf{g}_{k-1}\|_2 + L \|x_k - x_{k-1}\|_2 + \|\mathbf{g}_k\|_2 \end{aligned} \quad (26)$$

Because  $x_k = x_{k-1} - \alpha \hat{\mathbf{g}}_{k-1}$  we have that  $L \|x_k - x_{k-1}\|_2 \leq \alpha L \|\hat{\mathbf{g}}_{k-1}\|_2$ . Moreover, one can easily show that:

$$\|\mathbf{g}_{k-1}\|_2 \leq \frac{1}{1 - \varepsilon_{\text{rel}}} \|\hat{\mathbf{g}}_{k-1}\|_2$$

Thus equation (26) becomes

$$\begin{aligned} \|\hat{\mathbf{g}}_{k-1}\|_2 &\leq \frac{\varepsilon_{\text{rel}}}{1 - \varepsilon_{\text{rel}}} \|\hat{\mathbf{g}}_{k-1}\|_2 + \alpha L \|\hat{\mathbf{g}}_{k-1}\|_2 + \|\mathbf{g}_k\|_2 \\ \Rightarrow \left( \frac{1 - \alpha L - \varepsilon_{\text{rel}}(2 - \alpha L)}{1 - \varepsilon_{\text{rel}}} \right) \|\hat{\mathbf{g}}_{k-1}\|_2 &\leq \|\mathbf{g}_k\|_2 \end{aligned}$$

and so to guarantee (25), it suffices to choose

$$\begin{aligned}\delta_k &\leq \frac{2(\varepsilon_{\text{rel}} - \psi - \rho^n)(1 - L\alpha - \varepsilon_{\text{rel}}(2 - \alpha L))}{\tau H(1 - \varepsilon_{\text{rel}})} \|\hat{\mathbf{g}}_{k-1}\|_2 \\ &=: \beta \|\hat{\mathbf{g}}_{k-1}\|_2.\end{aligned}$$

Note that this condition is only meaningful when  $\beta > 0$ , thus we require that:

$$\psi + \rho^n < \varepsilon_{\text{rel}} < \frac{1 - \alpha L}{2 - \alpha L} \quad \text{and} \quad \alpha < \frac{1}{L}$$

□

Theorem 5.1 requires that  $\|\mathbf{g}_0 - \hat{\mathbf{g}}_0\|_2 \leq \varepsilon_{\text{rel}} \|\mathbf{g}_0\|_2$ . Let us briefly discuss how one can guarantee this. From Theorem A.4 we get that with probability  $1 - e^{-m/24}$ :

$$\begin{aligned}\|Z(\mathbf{g}_0 - \hat{\mathbf{g}}_0)\|_2^2 &\geq \frac{1}{2} \|\mathbf{g}_0 - \hat{\mathbf{g}}_0\|_2^2 \\ \Rightarrow \|\mathbf{g}_0 - \hat{\mathbf{g}}_0\|_2 &\leq \sqrt{2} \|Z\mathbf{g}_0 - Z\hat{\mathbf{g}}_0\|_2 \\ &\stackrel{(a)}{=} \sqrt{2} \|(\mathbf{y} + \delta\boldsymbol{\nu}) - Z\hat{\mathbf{g}}_0\|_2 \\ &\stackrel{(b)}{\leq} \sqrt{2} \left( \|\mathbf{y} - Z\hat{\mathbf{g}}_0\|_2 + \frac{H\delta}{2} \right)\end{aligned}$$

Where (a) follows from (15) with  $\sigma = 0$  and (b) follows from Lemma A.6. On the other hand:

$$\begin{aligned}\|\mathbf{y}\|_2 &\stackrel{(a)}{=} \|Z\mathbf{g}_0 + \delta\boldsymbol{\nu}\|_2 \\ &\stackrel{(b)}{\leq} \|Z\mathbf{g}_0\|_2 + \frac{H\delta}{2} \\ &\stackrel{(c)}{\leq} \sqrt{2} \|\mathbf{g}_0\|_2 + \frac{H\delta}{2},\end{aligned}$$

where again (a) follows from (15) and (b) from Lemma A.6 while (c) holds with probability  $1 - e^{-m/12}$  by Theorem A.4. It follows that:

$$\frac{1}{\sqrt{2}} \left( \|\mathbf{y}\|_2 - \frac{H\delta}{2} \right) \leq \|\mathbf{g}_0\|_2$$

and thus if:

$$\begin{aligned}\sqrt{2} \left( \|\mathbf{y} - Z\hat{\mathbf{g}}_0\|_2 + \frac{H\delta}{2} \right) &\leq \frac{\varepsilon_{\text{rel}}}{\sqrt{2}} \left( \|\mathbf{y}\|_2 - \frac{H\delta}{2} \right) \\ \iff \|\mathbf{y} - Z\hat{\mathbf{g}}_0\|_2 &\leq \frac{\varepsilon_{\text{rel}}}{2} \|\mathbf{y}\|_2 - \left( 1 + \frac{\varepsilon_{\text{rel}}}{2} \right) \left( \frac{H\delta}{2} \right),\end{aligned}$$

then with probability  $1 - e^{-m/12} - e^{-m/24}$  we indeed have that  $\|\mathbf{g}_0 - \hat{\mathbf{g}}_0\|_2 \leq \varepsilon_{\text{rel}} \|\mathbf{g}_0\|_2$ . This condition is checkable, assuming we have a good estimate of  $H$ . Furthermore, it must hold for  $\delta$  sufficiently small. Thus, we recommend starting with some initial estimate  $\delta_0$  and performing a decreasing binary search over  $(0, \delta_0)$  until a  $\delta$  is found such that this condition holds.

*Proof of Corollary 5.2. Part 1:* By assumption, we may choose  $\varepsilon_{\text{rel}}$  and  $n$  satisfying:

$$\psi + \rho^n < \varepsilon_{\text{rel}} < \frac{1 - \alpha L}{2 - \alpha L}$$

hence by Theorem 5.1,  $\|\mathbf{g}_k - \hat{\mathbf{g}}_k\|_2 \leq \varepsilon_{\text{rel}} \|\mathbf{g}_k\|_2$  for all  $k$ . Since in addition  $\varepsilon_{\text{rel}} \leq (2 - L\alpha)/(4 - L\alpha)$ , from Theorem B.6,  $\|x_k - \mathbf{P}_*(x_k)\|_2 \leq R$  for some fixed  $R$ . The stated convergence rate then follows from Theorem 4.1.

**Part 2:** follows from combining Theorems 5.1 and 4.2.  $\square$

*Proof of Theorem 5.3.* Appealing again to Theorem 3.2, this time with  $\sigma = 0$  and  $\psi = 0$ , we get

$$\|\mathbf{g}_k - \hat{\mathbf{g}}_k\|_2 \leq \frac{\tau \delta_k H}{2} + \rho^n \|\mathbf{g}_k\|_2$$

for all  $k$ . Because  $\mathbf{g}_k$  is  $s$ -sparse:

$$\begin{aligned} \|\mathbf{g}_k\|_2 &\stackrel{(a)}{\leq} \frac{1}{\sqrt{1 - \delta_s(Z)}} \|Z \mathbf{g}_k\|_2 \\ &\stackrel{(b)}{\leq} \frac{1}{\sqrt{1 - \delta_s(Z)}} (\|\mathbf{y}_k\|_2 + \delta_k \|\boldsymbol{\nu}\|_2) \\ &\stackrel{(c)}{\leq} \frac{1}{\sqrt{1 - \delta_s(Z)}} \left( \|\mathbf{y}_k\|_2 + \frac{\delta_k H}{2} \right) \\ &\stackrel{(d)}{\leq} \sqrt{2} \left( \|\mathbf{y}_k\|_2 + \frac{\delta_k H}{2} \right) \end{aligned}$$

where (a) follows from the definition of the RIP (see discussion below Theorem A.1), (b) follows from (15), (c) follows from Lemma A.6 and (d) is because  $\delta_s(Z) \leq \delta_{4s}(Z) \leq 0.5$  by Theorem A.1.

Choosing  $n$  sufficiently large (specifically  $n = \frac{\log(\delta_k H/2) - \log(\sqrt{2}(\|\mathbf{y}\|_k + \delta_k H/2))}{\log(\rho)}$ ) we obtain:

$$\|\mathbf{g}_k - \hat{\mathbf{g}}_k\|_2 \leq \frac{\tau \delta_k H}{2} + \frac{\tau \delta_k H}{2} \leq \frac{C \tau H}{k^{1.1}}$$

given the choice of  $\delta_k$ .  $\square$

*Proof of Corollary 5.4.* Apply Theorem 5.3 and Proposition 1 of (Schmidt et al., 2011). Note that by Theorem 5.3

$$\sum_{k=1}^{\infty} \|\mathbf{g}_k - \hat{\mathbf{g}}_k\|_2 \leq \tau H C \sum_{k=1}^{\infty} k^{-1.1} = E_{\infty}$$

$\square$

*Proof of Theorem 5.5.* From Theorem 3.2 we obtain:

$$\|\mathbf{g}_k - \hat{\mathbf{g}}_k\|_2 \leq \frac{2\tau\sigma}{\delta} + \frac{\tau\delta H}{2} + \rho^n \|\mathbf{g}_k\|_2$$

with probability  $1 - (s/d)^{O(s)}$ . Using the same trick as in the proof of Theorem 5.3 we can guarantee that  $\|\mathbf{g}_k\|_2 \leq \tau\delta_k H/2$  for  $n$  sufficiently large and so:

$$\|\mathbf{g}_k - \hat{\mathbf{g}}_k\|_2 \leq \frac{2\tau\sigma}{\delta} + \tau\delta H$$

Optimizing the right hand side in terms of  $\delta$  we obtain that  $\|\mathbf{g} - \hat{\mathbf{g}}\|_2 \leq 2\sqrt{2\tau\sigma H}$  and that this is achieved when  $\delta = \sqrt{2\sigma/H}$   $\square$

*Proof of Corollary 5.6.* From Theorem 5.5, we get that  $\|\mathbf{g}_k - \hat{\mathbf{g}}_k\|_2 \leq 2^{3/2}\sqrt{\tau\sigma H}$  for all  $k = 1, \dots, K$  with probability  $1 - (s/d)^{O(s)}$ . The first claim follows by combining this with Theorem 4.1 part 1. Note that  $\|x_k - P_*(x_k)\|_2 \leq R$  for all  $k$  by Theorem B.6 part 2. The second claim follows from combining the estimate  $\|\mathbf{g}_k - \hat{\mathbf{g}}_k\|_2 \leq 2^{3/2}\sqrt{\tau\sigma H}$  with Theorem 4.2 part 1.  $\square$

*Proof of Corollary 5.7.* This again follows from Proposition 1 of (Schmidt et al., 2011), combined with Theorem 5.5. Note that here  $\sum_{k=1}^K \frac{\|\mathbf{g}_k - \hat{\mathbf{g}}_k\|_2}{L} = \frac{2K\sqrt{2\tau\sigma H}}{L}$ .  $\square$

*Proof of Theorem 5.8.* By the assumptions on  $\|\mathbf{g}_0 - \hat{\mathbf{g}}_0\|_2$  and the fact that  $\varepsilon_{\text{rel}} < \min_{i:(g_0)_i \neq 0} |(g_0)_i|/\|\mathbf{g}_0\|_2$  we have that:

$$\min_{i:(g_0)_i \neq 0} |(g_0)_i| > \|\mathbf{g}_0 - \hat{\mathbf{g}}_0\|_2 \Rightarrow \hat{S}_0 := \text{supp}(\hat{\mathbf{g}}_0) = \text{supp}(\mathbf{g}_0) =: S.$$

Now assume that  $\hat{S}_{k-1} = S$ . We claim that Algorithm 4 will return  $\hat{\mathbf{g}}_k$  satisfying  $\hat{S}_k := \text{supp}(\hat{\mathbf{g}}_k) = S$  and  $\|\mathbf{g}_k - \hat{\mathbf{g}}_k\|_2 \leq \varepsilon_{\text{rel}}\|\mathbf{g}_k\|_2$  while making only  $s$  oracle queries. To see this, let  $Z_S$  denote the submatrix of  $Z$  containing only the columns indexed by  $S$ . Observe that  $Z_S$  is invertible, almost surely, and that  $\lambda_{\min}(Z_S) \geq \varepsilon_{\text{inv}}/\sqrt{s}$  with probability at least  $1 - O(\varepsilon_{\text{inv}})$  (see Theorem A of (Tikhomirov, 2020)). Let  $\hat{\mathbf{g}}$  be the solution to the support-constrained least squares problem in line 5 of Algorithm 4. Then:

$$[\hat{\mathbf{g}}]_S = Z_S^{-1} \mathbf{y} = Z_S^{-1} (Z\mathbf{g}_k + \delta\sqrt{s}\boldsymbol{\nu}).$$

Using (15). Note the discrepancy here: in (15)  $\boldsymbol{\nu} \in \mathbb{R}^m$  whereas here  $\boldsymbol{\nu} \in \mathbb{R}^s$  and has entries  $\nu_i = z_i^\top \nabla^2 f(x + tz_i) z_i / \sqrt{s}$  for some  $t \in (0, 1)$ . Continuing:

$$\begin{aligned} [\hat{\mathbf{g}}]_S &= Z_S^{-1} (Z_S[\mathbf{g}_k]_S + \delta\sqrt{s}\boldsymbol{\nu}) \quad (\text{As } \text{supp}(\mathbf{g}_k) = S) \\ &= [\mathbf{g}_k]_S + \delta\sqrt{s}Z_S^{-1}\boldsymbol{\nu}. \end{aligned}$$

Hence,  $\|Z\hat{\mathbf{g}} - \mathbf{y}\|_2 = 0$  and  $\hat{\mathbf{g}}$  is always accepted as the output of Algorithm 4 in lines 6–8 (*i.e.*  $\hat{g}_k = \hat{g}$ ). Thus indeed Algorithm 4 makes  $s$  oracle queries, and by construction  $\text{supp}(\hat{\mathbf{g}}_k) = S$ . Moreover:

$$\|\hat{\mathbf{g}} - \mathbf{g}_k\|_2 \leq \delta\sqrt{s}\|Z_S^{-1}\boldsymbol{\nu}\|_2 \leq \delta\sqrt{s}\|Z_S^{-1}\|_2\|\boldsymbol{\nu}\|_2 \leq \delta\sqrt{s}(\lambda_{\min}(Z_S))^{-1} \frac{H}{2} \leq \delta \frac{sH}{2\varepsilon_{\text{inv}}},$$

where the last inequality holds with probability at least  $1 - O(\varepsilon_{\text{inv}})$ . As in the proof of Theorem 3.2 we obtain:

$$\left( \frac{1 - \alpha L - \varepsilon_{\text{rel}}(2 - \alpha L)}{1 - \varepsilon_{\text{rel}}} \right) \|\hat{\mathbf{g}}_{k-1}\|_2 \leq \|\mathbf{g}_k\|_2$$



and hence with the choice of  $\beta$  stated we get that:

$$\|\hat{\mathbf{g}} - \mathbf{g}_k\|_2 \leq \varepsilon_{\text{rel}} \|\mathbf{g}_k\|_2 \quad \text{for all } k, \text{ with probability at least } 1 - O(\varepsilon_{\text{inv}}). \quad (27)$$

Note that because  $\varepsilon < (1 - L\alpha)/(2 - L\alpha)$  we have that  $\beta > 0$ . Because  $\varepsilon_{\text{rel}} \leq (2 - L\alpha)/(4 - L\alpha)$  it again follows from Theorem B.6,  $\|x_k - P_*(x_k)\|_2 \leq R$  for some fixed  $R$ . Now appealing to Part 2 of Theorem 4.1 with  $K = T/s$ , we get that:

$$e_K \leq \frac{c_5 e_0 R^2}{T e_0 / c_1 s + c_5 R^2} = O\left(\frac{s}{T}\right).$$

□

## D More Numerical Results

### D.1 Synthetic example

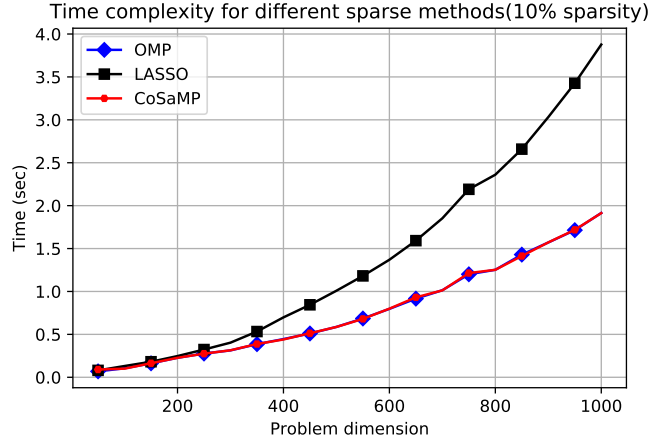


Figure 5: Running time *v.s.* problem dimension for different sparse methods when the sparsity ratio is fixed.

We investigate the runtime of ZORO with different sparse gradient estimators (*i.e.*, estimating the sparse gradients with OMP, LASSO or CoSaMP). The experiments are executed in MATLAB R2019a on a Windows 10 laptop with Intel i7-8750H CPU (6 cores at 2.2GHz) and 32GB of RAM. We implement all three versions of ZORO by ourselves. In particular, for the LASSO based gradient estimator, we use FISTA to be solver, and choose the regularizing parameter  $\lambda_{k+1}$  at  $(k+1)$ -th iteration by the ratio of the  $\ell_2$  residual squared and  $\ell_1$ -norm from the last iteration:  $\lambda_{k+1} = c \|\mathbf{y}_k - Z_k \hat{\mathbf{g}}_k\|_2^2 / \|\hat{\mathbf{g}}_k\|_1$ , where  $c$  is a fixed parameter throughout all iterations. Furthermore, the stop criteria of all three gradient estimators are set to  $\|x_{k+1} - x_k\|_2 / \|x_k\|_2 \leq 10^{-6}$ .

We consider the problem of minimizing a quadratic function  $f(x) = x^\top A x / 2$ , where  $A \in \mathbb{R}^{d \times d}$  is a diagonal matrix with  $s$  non-zero randomly generated positive elements. The runtime is evaluated with varying problem dimension (see Figure 5) and sparsity level (see Figure 6). Moreover, the

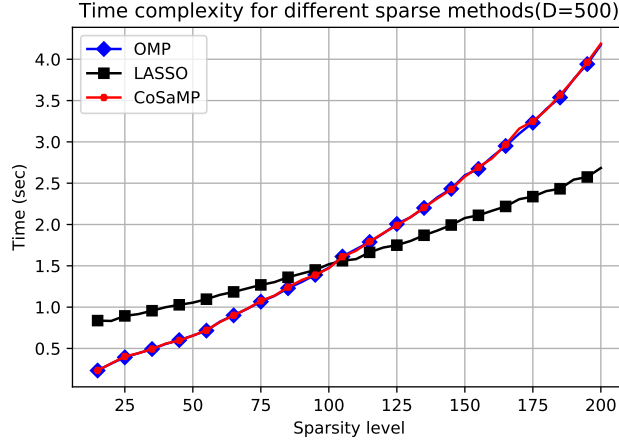


Figure 6: Running time *v.s.* sparsity level for different sparse methods when the the problem dimension is fixed.

runtimes reported in Figures 5 and 6 are based on 30 iterations of gradient descent, and averaged over 10 random tests. We find that the greedy methods, CoSaMP and OMP, have a speed advantage when the problem dimension is large and sparsity level is small, while the LASSO solver is fastest when both  $d$  and  $s$  are small. We emphasize that the gradients estimated by all three methods offer almost identical convergence performance on these easier synthetic tasks, so the stopping criterion of ZORO will not affect our observations.

## D.2 Sparse adversarial attack on ImageNet

For this numerical experiment, we use the code from <https://github.com/KaidiXu/ZO-AdaMM> with a few modifications. We focus on the per-image untargeted attack scenario. For the objective function, we change the  $\ell_2$ -norm of distortion to  $\ell_0$ -norm. At each iteration, we randomly select a subspace of 2000 variables and generate 50 random Rademacher perturbation signals in this subspace. We use a much larger step-size than (Chen et al., 2019) since our gradient estimate has much better precision. Note that there are several hyper-parameters (step-size, decay parameter, subspace dimension, ZORO parameters, etc.) that have not been fully optimized. We plan to address this issue along with more diverse simulation settings (targeted attacks, universal attacks, etc.) in a future work. We present some examples of successful sparse attack by ZORO in Figure 7.

Notice that the distortions are similar with impulse noise, which can be mitigated by a median filter. We use the tool `ndimage.median_filter` from `scipy`. We use  $\mathcal{A}$  to denote the set of adversarial images (original image+distortion) that are successfully attacked by ZORO. We use  $\mathcal{I}_1$  to denote the set of image IDs that are not recovered. The ratio of images in  $\mathcal{A}$  been identified to the true label after filtering is the recover successful rate:  $1 - |\mathcal{I}_1|/|\mathcal{A}|$ . We then analyze the side-effect of median filter by apply it to the original images of  $\mathcal{A}$ . We use  $\mathcal{I}_2$  to denote the set of image IDs that are mis-classified. The distortion rate is the ratio of images been assigned an incorrect label:  $|\mathcal{I}_2|/|\mathcal{A}|$ . We summarize the images indexes from these two experiments and calculate the total accuracy reduction:  $|\mathcal{I}_1 \cup \mathcal{I}_2|/|\mathcal{A}|$ . Note that there are some overlapping IDs in  $\mathcal{I}_1$  and  $\mathcal{I}_2$ .



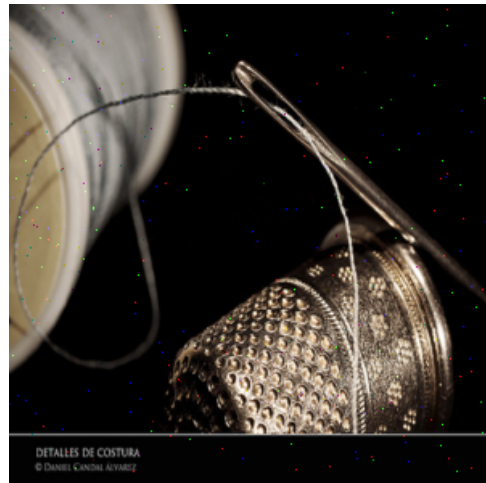
(a) True label: “corn” → Mislabeled: “ear, spike, capitulum”



(b) True label: “plastic bag” → Mislabeled: “shower cap”



(c) True label: “water ouzel, dipper” → Mislabeled: “otter”



(d) True label: “thimble” → Mislabeled: “measuring cup”

Figure 7: Examples of adversarial images and the mis-classified labels.